Fission barriers at the end of the chart of the nuclides

Peter Möller,[1,*] Arnold J. Sierk,[1] Takatoshi Ichikawa,[2] Akira Iwamoto,[3] and Matthew Mumpower[4]
[1]*Theoretical Division, Los Alamos National Laboratory, Los Alamos, New Mexico 87545, USA*
[2]*Yukawa Institute for Theoretical Physics, Kyoto University, Kyoto 606-8502, Japan*
[3]*Advanced Science Research Center, Japan Atomic Energy Agency (JAEA), Tokai-mura, Naka-gun, Ibaraki 319-1195, Japan*
[4]*Joint Institute for Nuclear Astrophysics, University of Notre Dame, 225 Nieuwland Science Hall, Notre Dame, Indiana 46556, USA*
(Received 2 July 2014; revised manuscript received 20 November 2014; published 12 February 2015)

We present calculated fission-barrier heights for 5239 nuclides for all nuclei between the proton and neutron drip lines with $171 \leqslant A \leqslant 330$. The barriers are calculated in the macroscopic-microscopic finite-range liquid-drop model with a 2002 set of macroscopic-model parameters. The saddle-point energies are determined from potential-energy surfaces based on more than 5 000 000 different shapes, defined by five deformation parameters in the three-quadratic-surface shape parametrization: elongation, neck diameter, left-fragment spheroidal deformation, right-fragment spheroidal deformation, and nascent-fragment mass asymmetry. The energy of the ground state is determined by calculating the lowest-energy configuration in both the Nilsson perturbed-spheroid (ϵ) and the spherical-harmonic (β) parametrizations, including axially asymmetric deformations. The lower of the two results (correcting for zero-point motion) is defined as the ground-state energy. The effect of axial asymmetry on the inner barrier peak is calculated in the (ϵ,γ) parametrization. We have earlier benchmarked our calculated barrier heights to experimentally extracted barrier parameters and found average agreement to about 1 MeV for known data across the nuclear chart. Here we do additional benchmarks and investigate the qualitative and, when possible, quantitative agreement and/or consistency with data on β-delayed fission, isotope generation along prompt-neutron-capture chains in nuclear-weapons tests, and superheavy-element stability. These studies all indicate that the model is realistic at considerable distances in Z and N from the region of nuclei where its parameters were determined.

DOI: 10.1103/PhysRevC.91.024310 PACS number(s): 24.75.+i, 25.85.Ec, 26.30.Hj, 21.60.−n

I. INTRODUCTION

In actinide fission a nucleus typically evolves from a single nucleus in its deformed ground state to two separated fragments: one large roughly spherical fragment with nucleon number $A \approx 140$ and a smaller deformed fragment with the remainder of the nucleons. In Ref. [1] we presented calculations of fission potential-energy surfaces and associated barrier heights for 1585 nuclei and some conclusions based on these studies. We now extend the study and tabulate barriers for 5239 nuclides in the region $171 \leqslant A \leqslant 330$ for all nuclei between the proton and neutron drip lines. All aspects of the calculations are identical to those presented in Ref. [1], where full details are given. However, we review both some important ingredients and features of our approach and how it is positioned with respect to other fission-barrier calculations. An overview of the results is presented in Figs. 1 and 2.

We have previously made the case that to study the nuclear potential energy during the shape evolution in fission and to allow the nucleus freedom to evolve into fragments with different shapes and into different fragment mass divisions, it is necessary to calculate the nuclear potential energy as a function of, at a minimum, five shape degrees of freedom corresponding to elongation, neck radius, left-fragment shape, right-fragment shape, and the asymmetry of the mass division [1–5]. It is also necessary to space the deformation points fairly densely so that shell-structure features appear accurately in the calculated potential-energy surfaces. As an example, consider the shell-structure effects in the tinlike fragment with $A \approx 140$. In ground-state mass calculations in which the associated microscopic corrections are also tabulated, for example in the FRDM(1992) mass calculation [6], we find that the ground-state microscopic corrections for $^{132}_{50}\mathrm{Sn}_{82}$, $^{130}_{50}\mathrm{Sn}_{80}$, and $^{130}_{48}\mathrm{Cd}_{82}$ are −11.55, −9.14, and −9.85 MeV, respectively. Thus, near magic numbers a change by one nucleon changes the microscopic correction by about 1 MeV. See Ref. [6] for precise definitions of the shell-plus-pairing correction and the associated microscopic correction. The latter quantity is a sum of the shell-plus-pairing correction, the deformation change of the macroscopic energy relative to the sphere and a zero-point energy. We therefore space our asymmetry coordinate so that one step in the asymmetry coordinate corresponds to moving about one proton and one neutron from one fragment to the other. For example, for an $A = 200$ nucleus the symmetric configuration obviously corresponds to a mass division $M_{\mathrm{H}}/M_{\mathrm{L}} = 100/100$ and our next grid point in the asymmetry coordinate corresponds to $M_{\mathrm{H}}/M_{\mathrm{L}} = 102/98$, where M_{H} is the heavy-fragment mass and M_{L} is the light-fragment mass. To allow studies of cold-fusion heavy-ion reactions on $^{208}_{82}\mathrm{Pb}_{126}$ targets leading to superheavy elements, we use 35 grid points in the asymmetry coordinate [1]. In the elongation coordinate Q_2 we use 45 grid points; in the remaining three deformation coordinates, we use 15 in each. This leads to more than 5 000 000 shapes. It should be obvious, but is perhaps not immediately intuitively clear, that the consequence is large data-storage needs. If the energy for each shape for each of the about 5000 nuclei is stored as a

*moller@lanl.gov

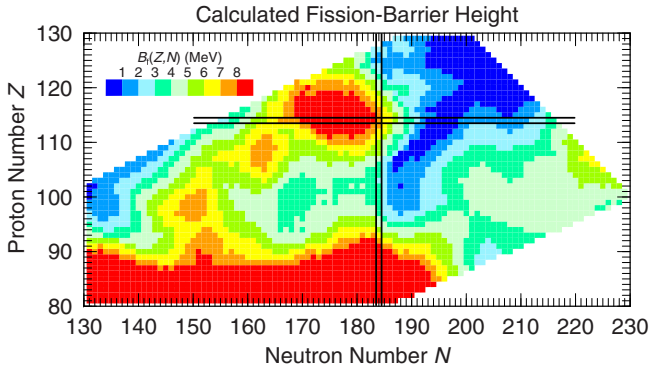

FIG. 1. (Color online) Calculated fission-barrier heights for 3282 nuclei. The highly variable structure is mostly due to ground-state shell effects. Ground-state shell effects are particularly strong in the deformed regions around $^{252}_{100}\mathrm{Fm}_{152}$ and $^{270}_{108}\mathrm{Hs}_{162}$ and in the nearly spherical region near the next doubly magic nuclide postulated to be at $^{298}_{114}\mathrm{Fl}_{184}$. Our strongest shell effects are slightly offset to the left with respect to this isotope.

ten-digit number, this means that the total data-storage space needed is $5\,000\,000 \times 10 \times 5\,000 = 2.5 \times 10^{11}$ bytes, which is 250 Gb of storage. When we started this type of calculation based on millions of shapes in 1999 [2], this was indeed a problem; now it is not.

II. OTHER FISSION POTENTIAL-ENERGY CALCULATIONS

In most previous fission studies various schemes were employed to avoid calculating a complete "hypercube" in all the deformation variables considered. Such complete calculations were impractical until computer performance had evolved sufficiently, roughly achieved around 1995–2000. In

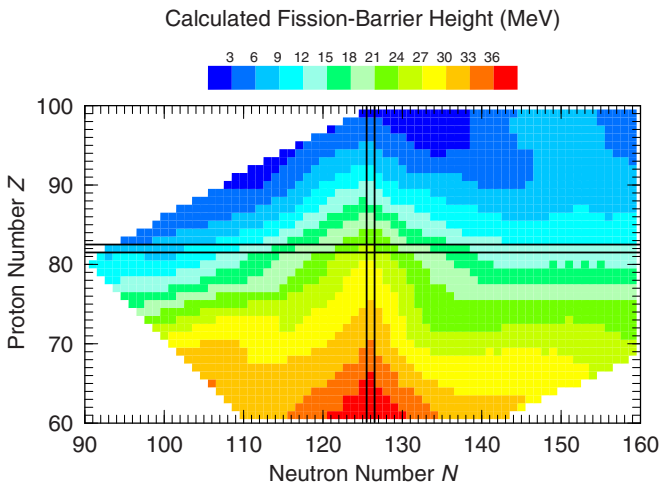

FIG. 2. (Color online) Calculated fission-barrier heights for 2113 nuclei with generally lower proton and neutron numbers than those in Fig. 1. Because the macroscopic energy contributes the major part of the fission-barrier height for most nuclei in this region, and because of the different energy scale compared to Fig. 1, the only shell effects clearly visible come from the $N = 126$ spherical neutron shell.

macroscopic-microscopic calculations it was the norm to plot energies versus two shape variables, for example β_2 and β_3 (quadrupole and octupole deformations), and "minimize" the potential energy with respect to additional multipoles; typical examples are Refs. [7,8]. Although such approaches intuitively seem promising, there are significant concerns about the uniqueness and stability of such results. First, when minimizations are carried out at a specific location (β_2,β_3), what are the starting values of the additional shape variables over which the minimization is carried out? A trivial suggestion is that the values obtained for a previous point be used, but which is the "previous point" will depend upon the sequence in which the grid points are considered. It is easy to visualize a surface, even in two dimensions, for which a different result may be found by approaching a particular point from opposite directions. Another strategy could be that the minimizations are started at the value zero of the additional variables at each point (β_2,β_3), but these approaches would miss possible multiple deformed minima. And, even if found, it would be impossible to display multiple minima versus the "hidden" shape variables in a two-dimensional contour plot. Furthermore, none of these methods, which only access a limited part of the higher-dimensional space, are guaranteed to find the true saddle points with reasonable accuracy. In some cases, the saddle solutions will be correct, but there is no way to mathematically evaluate the possible errors inside the model framework itself. In many of these minimization studies points that seem near each other in the two-dimensional (β_2,β_3) plots are actually quite distant in the higher-dimensional space. This is often manifested as strong discontinuities appearing in published potential-energy contour diagrams or plots of energy surfaces. Despite these known deficiencies, these methods are still in routine use today [9]. However, very recently other groups previously employing such approximations have come to the conclusion that the minimization method is deficient, not just in principle but also in practice. In one recent macroscopic-microscopic model study, the calculations were carried out for complete multidimensional "hypercubes" and they confirmed that the immersion methods we employ are crucial to avoiding spurious results from the use of minimization. It is stated directly, "*This shows that the minimization is an uncertain method of the search for saddles . . .*," in the summary conclusions [10].

Currently, the main alternative approach to macroscopic-microscopic calculations of fission-barrier potential-energy surfaces and saddle points is the constrained Hartree-Fock method introduced in 1973 [11]. Those authors state "*One of the advantages of this type of calculation is that deformation energy curves can be calculated without making a complete map of the deformation energy surface.*" Another comment that is often made in connection with determining fission saddle points is that "constrained self-consistent methods automatically take all higher shape degrees of freedom into account." However, these statements are misleading. Imposing shape constraints in self-consistent methods is mathematically equivalent to the use of minimization techniques in macroscopic-microscopic methods, which we, and now other groups, have demonstrated are flawed. A detailed discussion is in Ref. [1]. A very transparent discussion coming from outside

the field of nuclear physics is in Ref. [12]. The example used there is the determination of the Continental Divide in the United States, but this problem is essentially identical to that of finding saddle points in potential-energy surfaces, although easier to visualize because geographical topography is studied in two-dimensional spaces only.

It has been suggested that when constrained Hartree-Fock or Hartree-Fock-Bogoliubov calculations are presented, for example as two-dimensional contour maps, a *necessary* condition to impose on the results is that the spatial overlap between the wave functions for neighboring grid points in the contour plot should be large. If there exist neighbor points that do not fulfill a required overlap criterion, then one would need to go from two to three constraints, or, in the general case, add one additional constraint and again impose the continuity check [13]. But even if the potential energy obtained with two constraints corresponds to a continuous variation of the densities, it is by no means certain that a saddle point on this surface is a good approximation to the real (lowest) saddle point; see, for example, the discussion of Fig. 5 in Ref. [1]. Based on these observations of problems with existing alternative methods and the evidence from our multitude of benchmarks (see below), we feel that the approach we use is the most accurate currently available for large-scale calculations of databases of various fission-barrier properties.

III. SUMMARY OF ESSENTIAL MODEL FEATURES

In the macroscopic-microscopic model the energy for a specific, prescribed nuclear shape is calculated as a sum of a macroscopic energy and a microscopic shell-plus-pairing correction. In the community, several different models are used for the macroscopic and the microscopic parts. For example, the microscopic part can be based on a modified-oscillator (Nilsson) single-particle potential [14,15], a Woods-Saxon single-particle potential [16], a folded-Yukawa single-particle potential [17], or other potentials. We use what we have called the finite-range liquid-drop model (FRLDM) [18] for the macroscopic part and the folded-Yukawa single-particle model as the starting point for the microscopic part. When we refer to the full macroscopic-microscopic model, we for brevity use the notation FRLDM when the macroscopic part is the finite-range liquid-drop model and FRDM when the macroscopic part is based on the finite-range droplet model; we do not use the latter in our fission-barrier calculations, for reasons we explain below.

A. Macroscopic model

For the macroscopic energy we use the FRLDM. Briefly stated, it is based on a standard shape-dependent "liquid-drop" model [19,20], which is enhanced to take the finite range of the nuclear force [18] and the diffuseness of the charge distribution [21] into account. In the original liquid-drop model, the surface energy is strictly proportional to the surface area of the nucleus [22]. For shapes with well-developed small-radius necks, this leads to too high a surface-energy contribution to the macroscopic energy in the neck region. For such shapes the finite range of the attractive nuclear force may be thought of as reaching across the neck region to nucleons on the opposite side of the neck, leading to a reduction of the surface energy. The effect is also important in calculations of heavy-ion interaction barriers and even for some ground-state shapes containing higher-multipole components. An in-depth presentation of the model and discussions of these issues are found in Refs. [6,18,21].

When fission was discovered [23], it was realized that the observations could be interpreted in terms of a macroscopic, deformable liquid-drop model [24,25]. Bohr and Wheeler very soon afterward presented a quantitative description of the shape dependence of the surface and Coulomb energies in terms of Taylor expansions and obtained the systematics of fission-barrier heights for nuclei throughout the periodic system [22].

To model nuclear masses more accurately than was possible with the original liquid-drop model, or semiempirical mass model [26], phenomenological shell corrections with adjustable parameters were often added to the macroscopic expression. In these studies it was observed that in addition to a strong contribution from microscopic effects at and near magic numbers, it was necessary to account for the extra binding that was observed for nuclei with equal or nearly equal proton and neutron numbers [19]. One commonly used form for this "Wigner energy," which we use, is

$$E_{\mathrm{W}} = W\left[\frac{|N-Z|}{N+Z}\right], \tag{1}$$

where for the Wigner constant W, we use the value 30 MeV. In nuclear mass models this term was customarily included without a shape dependence. For a ^{236}U nucleus this contribution to the nuclear potential energy is 6.6 MeV. However, if we use the model to describe the highly deformed shapes in fission near the transition from a single shape to two fragments, it is relevant to ask if this shape-independent formulation makes sense. For example, for the simple case of two touching spheres we would hope to get the same calculated energy if we consider the system as one very deformed single shape or as two separate touching nuclei. Clearly, if we consider any division of the original nuclear system with proton and neutron numbers Z_{comp} and N_{comp} into two fragments (1) and (2) with proton and neutron numbers Z_1, N_1, Z_2, and N_2 while preserving neutron-proton asymmetry, that is,

$$Z_1 = \alpha \times Z_{\mathrm{comp}} \quad N_1 = \alpha \times N_{\mathrm{comp}} \quad \text{and}$$
$$Z_2 = (1-\alpha) \times Z_{\mathrm{comp}} \quad N_2 = (1-\alpha) \times N_{\mathrm{comp}},$$

where α is a fractional number in the range 0–1, then there will be a Wigner-energy contribution $E_{\mathrm{W}} = 6.6$ MeV to each of the touching nuclei. Thus, for the touching configuration there will be a difference of 6.6 MeV in calculated potential energy if it is treated as a scission configuration or as two touching nuclei. Obviously, for the touching configuration one would also need to take into account the interaction energies between the two nuclei. After doing this, to avoid this 6.6-MeV remaining discontinuity, it is necessary to introduce a shape

dependence for the Wigner energy, so that

$$E_{\mathrm{W}} = W\left[\frac{|N-Z|}{N+Z}\right]B_{\mathrm{W}}, \tag{2}$$

where the shape-dependent function B_{W} evolves continuously from $B_{\mathrm{W}} = 1$ for a shape with no discernible neck to $B_{\mathrm{W}} = 2$ as the shape evolves into separated fragments. These issues are further discussed in Ref. [27], where the exact expression we use for the deformation dependence of B_{W} is given. The specific functional form for this dependence is not derived, but is arbitrarily defined to smoothly transition from a value of 1 to a value of 2 as a function of the developing neck. Similar considerations show that it is necessary to introduce a shape dependence for the constant, "$a_o A^0$ term," that occurs in the FRLDM. The FRLDM used in our calculations is completely specified in Ref. [6] in Sec. 3.5, except that the above shape dependencies were not introduced. Thus, the constant and Wigner terms in Eq. (62) in Ref. [6] are generalized to

$$\begin{aligned} &E_{\mathrm{macr}}(Z,N,\mathrm{shape}) \\ &\quad = \cdots + a_0 A^0 B_{\mathrm{W}} \\ &\qquad + W\left(|I|B_{\mathrm{W}} + \begin{cases} 1/A, & Z \text{ and } N \text{ odd and equal} \\ 0, & \text{otherwise} \end{cases}\right)\cdots . \end{aligned} \tag{3}$$

Potential-energy calculations without and with these shape dependencies are shown in Fig. 3. The slight discontinuity in the "Total fusion" curve is mainly due to the equalization of the Fermi surfaces of the two colliding nuclei that occurs after contact.

Because, in our studies since the year 1999, we have calculated fission potential-energy surfaces for several million deformation-grid points, this has systematically lowered all calculated fission saddle-point energies compared to those calculated previously using a much smaller space of shapes. The macroscopic-model constants thus had to be readjusted by a simultaneous fit to experimental barrier heights and ground-state masses, leading to different macroscopic parameters from those in Ref. [6], referred to as FRLDM(1992). We now use the constants FRLDM(2002), given in Ref. [28].

We emphasize that in nuclear-mass calculations we obtain the most accurate results by use of the finite-range droplet model (FRDM). This model is a combination of the FRLDM and the droplet model [29], which allows, at a macroscopic level, calculation of effects of Coulomb redistribution (some charge is pushed from the center toward the surface) and other related effects. These effects lead to about a 15% improvement in mass-model accuracy. But the droplet model enhancement introduces many terms that are derived as expansions in terms of small deformations around a spherical shape. It is therefore not possible to take it to large deformations and make a continuous energy transition at scission to separated shapes using this macroscopic model. Therefore, it cannot be used in calculations of fission potential-energy surfaces. In our study of masses in Ref. [6] we actually performed a limited calculation of fission-barrier heights in the FRDM and the model parameters were determined by adjusting to a weighted sum of masses and barrier heights. At that time the barrier saddle points were determined from a 1973 calculation [30,31] in a three-dimensional space containing only 175 different shapes. The saddle shapes obtained in this calculation did not exhibit obvious neck indentations (and as we now realize were not very realistic [2,3]), so we did not address the issue that the droplet model and the FRDM become increasingly inaccurate at large deformations. This is why we now in fission calculations use only the FRLDM.

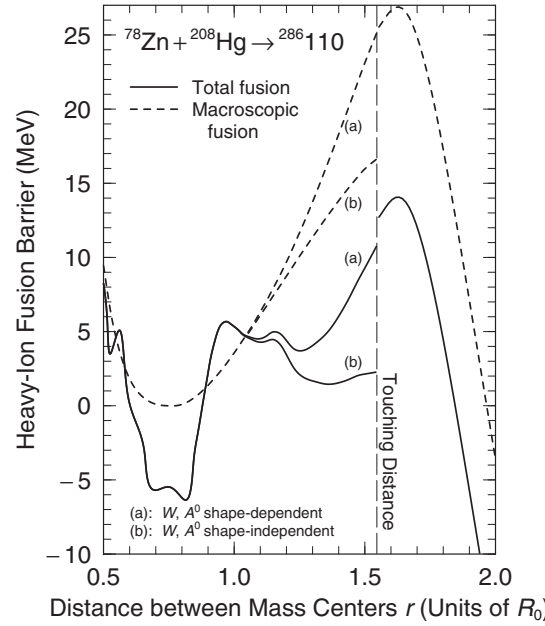

FIG. 3. Calculated macroscopic and total potential energies for shape sequences leading to the touching configuration, at the long-dashed line, of spherical ^{78}Zn and ^{208}Hg. To the left the calculations trace the energy for a *single, joined* shape configuration from oblate shapes through the spherical shape at $r = 0.75$ to the touching configuration at $r = 1.52$; to the right the calculations give the energy for separated spherical nuclei beyond the touching point. The continuous path through five-dimensional space from the ground state to the touching configuration is arbitrary; the key point is that the limiting shapes when approaching the line of touching from the left and right are identical, namely spherical ^{78}Zn and ^{208}Hg in contact. At a specific value of r all curves are calculated for the same shape. To obtain continuity of the macroscopic energy at touching, a crucial feature in realistic models, it is essential that various model terms depend appropriately on nuclear shape, as is the case for the curves (a). The slight remaining discontinuity in the *total* fusion energy curve (solid line) arises because the Fermi surfaces of the nuclei readjust at contact and because pairing and spin-orbit strength parameters also undergo small discontinuous changes there. This figure and caption are adapted from Ref. [28].

B. Microscopic model

The shell-plus-pairing corrections are calculated by use of Strutinsky's method from single-particle levels in a folded-Yukawa potential. The single-particle potential is almost unchanged since 1973 [17,32], except that in 1980, to permit application to the whole nuclear chart, we let the neutron and

proton spin-orbit strengths depend weakly on the nucleon number A [33]. The shell-plus-pairing corrections are calculated as described in Ref. [17] with the following enhancements. First, to avoid the well-known collapses of the BCS method, we now use a Lipkin-Nogami pairing model implemented as explained in detail in Ref. [34]. Again, imposing continuity at scission required that some constants of the Strutinsky and pairing models depend on deformation, which is discussed in detail in Refs. [6,27]. Full details of the current implementation of the microscopic model are given in Ref. [6], including values of all its constants and various shape dependencies, if any.

C. Deformation grid

Although many of the essential features of the macroscopic-microscopic model were developed up to 40 years ago, it is the continuous increase in computer power that has made it possible to exploit its full potential. In calculations 40 years ago, theoretical studies of mass asymmetry in fission had to be based on potential-energy surfaces calculated for only a very few shapes: for example, versus two independent deformation coordinates for 20 shapes in an early (1970) study [35] versus three independent shape coordinates for 175 shapes in 1973 [30]. The 1973 calculation took about 30 h on a CDC 6600 at Los Alamos Scientific Laboratory, a computer shared by hundreds of researchers. Both these (and other) calculations obtained mass-asymmetric outer saddle points but beyond the outer saddles the potential-energy contour plots developed the deepest "valley" for shapes corresponding to symmetric divisions, in apparent contradiction to experimentally observed asymmetric fragment splits. These results were dismissed by comments like "valleys are not invariant under coordinate transformation" [30] (an observation originally emphasized by Wilets [36]) or that dynamics determined the final outcome. However, the asymmetry in actinide fission was almost since its discovery explained in a hand-waving fashion as due to a preference of the system to divide into one fragment as close as possible to the spherical, doubly magic ^{132}Sn nucleus and a remainder, a smaller, deformed fragment. Thus, to permit the potential energy to contain all deformation features related to such divisions one needs to calculate the potential, as stated previously, versus at least five shape degrees of freedom: elongation, neck radius, the two nascent-fragment shapes, and mass asymmetry. In the three-quadratic-surface parametrization one can by suitable manipulations of the expressions involved (see Ref. [1]) use these variables, which have an obvious intuitive interpretation, to specify the deformation grid. Also, in this grid the five different shape coordinates are, loosely speaking, nearly orthogonal, which permits a quick, intuitive interpretation of the calculated five-dimensional potential-energy surfaces. Recently we have also shown that calculations of fission-fragment yields based on a simple "random walk" in this five-dimensional space and the Metropolis algorithm gives excellent agreement with experimental data [37–39]. This suggests two conclusions. First, the coordinate choice and spacing is quite consistent with intuitive interpretations; otherwise, it would not have been possible to interpret in a straightforward fashion the features of the potential-energy surface in terms of symmetric and asymmetric valleys, different saddle points leading into these different valleys, and ridges in between [1,5], nor would the Metropolis algorithm have given as realistic results as it now does. Second, we can conclude, because the yield calculations reproduce the substantial differences between the ^{236}U and ^{240}Pu yields [37] that the calculated potential energy is realistic also beyond the outer saddle points, which had not been clearly established earlier, although some hints had been seen in calculations of the most-probable mass divisions [5]. The algebra that is involved in taking the above intuitive coordinate concepts into the actual expressions that in the three-quadratic-surface parametrization generate these shapes is rather tedious and we therefore direct the reader to Ref. [1] for details.

Axially asymmetric deformations are also investigated, but these studies are limited to the ground state and the inner-barrier saddle point. Since the three-quadratic-surface shapes are not able to generate optimal ground-state shapes for some nuclei, we have furthermore calculated ground-state energies in the ϵ and β parametrizations. Again, the precise definitions of the deformation grids in these three additional potential-energy calculations are given in Ref. [1], where also details on how the barrier heights are extracted based on the combined information contained in these four complementary potential-energy surfaces are given.

IV. RESULTS

We have calculated barrier heights B_f for 5239 nuclides exactly as described in Ref. [1] and references cited therein. We have summarized the model features in the section above, in particular facts and features that might be somewhat time consuming to trace in a quick scan of the references. The barriers are tabulated in Table I.

The fission-barrier properties of our model have previously been benchmarked with respect to known data for nuclides near β-stability. We have shown that we reproduce the outer barrier-peak height for 31 nuclides from $^{70}_{34}\mathrm{Se}_{36}$ to $^{252}_{98}\mathrm{Cf}_{154}$ with an rms deviation of only 1.0 MeV [28]. We have also compared calculated actinide inner and outer barrier heights as well as the height of the fission-isomer minimum to barrier parameters extracted from various types of experimental data, often cross sections as functions of energy for neutron-induced fission [1]. In this context we observe that the "experimental" barrier parameters are not as directly measured data as, for example, nuclear masses are in some experiments. The "experimental" barrier parameters are numbers occurring in models of experimental cross sections. Moreover, these models almost always assume one-dimensional barriers, whereas our barrier parameters refer to saddles and minima in five-dimensional deformation spaces. Further complicating the situation is that different evaluations (of different sets of experimental data and/or just using different cross-section models) often lead to different results for the extracted barrier parameters. For example, Blons and collaborators [40] consistently find that the so-called "third minima" of some light actinide nuclei are very shallow and no more than 0.5 MeV or so below the surrounding second and third barrier peaks, which are about

TABLE I. Calculated fission-barrier heights.

N	A	B_f (MeV)	N	A	B_f (MeV)	N	A	B_f (MeV)	N	A	B_f (MeV)	N	A	B_f (MeV)	N	A	B_f (MeV)
$Z = 51$ (Sb)			$Z = 56$ (Ba)			$Z = 58$ (Ce)			$Z = 60$ (Nd)			$Z = 62$ (Sm)			$Z = 63$ (Eu)		
120	171	42.48	122	178	40.39	133	191	35.72	132	192	35.02	118	180	33.70	134	197	31.75
121	172	43.34	123	179	41.29	134	192	35.01	133	193	34.46	119	181	34.11	135	198	31.29
$Z = 52$ (Te)			124	180	41.75	135	193	34.02	134	194	33.43	120	182	34.47	136	199	30.83
119	171	41.24	125	181	43.23	136	194	33.09	135	195	32.65	121	183	35.41	137	200	30.83
120	172	41.73	126	182	43.36	137	195	32.25	136	196	31.85	122	184	35.94	138	201	30.55
121	173	42.63	127	183	42.27	$Z = 59$ (Pr)			137	197	32.09	123	185	36.97	139	202	30.50
122	174	43.12	128	184	41.25	112	171	33.38	138	198	31.61	124	186	37.62	140	203	30.25
123	175	43.87	129	185	39.85	113	172	33.74	139	199	30.94	125	187	38.94	141	204	30.34
124	176	44.38	130	186	38.40	114	173	33.91	140	200	30.76	126	188	39.36	142	205	30.37
$Z = 53$ (I)			131	187	37.68	115	174	34.32	141	201	30.58	127	189	38.37	143	206	30.39
118	171	40.35	132	188	36.74	116	175	34.61	$Z = 61$ (Pm)			128	190	37.42	144	207	30.24
119	172	41.42	133	189	36.60	117	176	35.62	110	171	32.33	129	191	36.23	145	208	30.04
120	173	41.76	$Z = 57$ (La)			118	177	36.09	111	172	32.25	130	192	35.28	146	209	29.70
121	174	42.43	114	171	35.64	119	178	36.76	112	173	32.25	131	193	34.85	147	210	29.56
122	175	42.68	115	172	36.24	120	179	37.19	113	174	32.54	132	194	33.81	148	211	29.37
123	176	43.56	116	173	36.81	121	180	38.03	114	175	32.62	133	195	33.16	$Z = 64$ (Gd)		
124	177	43.98	117	174	37.36	122	181	38.50	115	176	32.91	134	196	32.07	107	171	32.85
125	178	45.53	118	175	37.79	123	182	39.57	116	177	33.10	135	197	31.44	108	172	32.49
126	179	45.87	119	176	38.61	124	183	40.13	117	178	33.84	136	198	31.00	109	173	32.33
$Z = 54$ (Xe)			120	177	39.04	125	184	41.47	118	179	34.27	137	199	30.93	110	174	31.92
117	171	38.87	121	178	39.79	126	185	41.88	119	180	35.04	138	200	30.66	111	175	31.71
118	172	39.50	122	179	40.18	127	186	40.92	120	181	35.28	139	201	30.52	112	176	31.47
119	173	40.40	123	180	41.01	128	187	39.73	121	182	36.40	140	202	30.26	113	177	31.30
120	174	40.77	124	181	41.50	129	188	38.62	122	183	36.83	141	203	30.29	114	178	31.27
121	175	41.43	125	182	42.90	130	189	37.41	123	184	37.96	142	204	30.33	115	179	31.72
122	176	41.72	126	183	43.20	131	190	36.98	124	185	38.61	143	205	30.33	116	180	31.66
123	177	42.51	127	184	42.20	132	191	36.05	125	186	40.01	144	206	30.23	117	181	32.20
124	178	42.94	128	185	40.94	133	192	35.47	126	187	40.36	145	207	29.96	118	182	32.59
125	179	44.48	129	186	39.77	134	193	34.50	127	188	39.42	146	208	29.63	119	183	33.06
126	180	44.73	130	187	38.41	135	194	34.11	128	189	38.44	$Z = 63$ (Eu)			120	184	33.53
127	181	43.46	131	188	37.79	136	195	33.15	129	190	37.31	108	171	32.51	121	185	34.13
128	182	42.04	132	189	36.97	137	196	32.54	130	191	36.28	109	172	32.61	122	186	34.52
$Z = 55$ (Cs)			133	190	36.61	138	197	31.96	131	192	35.87	110	173	31.96	123	187	35.37
116	171	38.23	134	191	35.39	139	198	31.33	132	193	34.87	111	174	31.87	124	188	35.91
117	172	38.95	135	192	34.28	$Z = 60$ (Nd)			133	194	34.23	112	175	31.62	125	189	37.25
118	173	39.34	$Z = 58$ (Ce)			111	171	32.65	134	195	33.15	113	176	31.80	126	190	37.70
119	174	40.13	113	171	34.22	112	172	32.73	135	196	32.48	114	177	31.67	127	191	36.64
120	175	40.44	114	172	34.49	113	173	32.98	136	197	31.89	115	178	31.98	128	192	35.74
121	176	41.34	115	173	35.20	114	174	33.24	137	198	31.82	116	179	32.15	129	193	34.77
122	177	41.47	116	174	35.47	115	175	33.50	138	199	31.43	117	180	32.66	130	194	33.84
123	178	42.31	117	175	36.41	116	176	33.73	139	200	31.15	118	181	33.01	131	195	33.45
124	179	42.71	118	176	36.76	117	177	34.54	140	201	30.91	119	182	33.62	132	196	32.43
125	180	44.24	119	177	37.42	118	178	35.10	141	202	30.78	120	183	34.06	133	197	31.80
126	181	44.51	120	178	37.81	119	179	35.83	142	203	30.74	121	184	34.93	134	198	30.83
127	182	43.33	121	179	38.62	120	180	36.02	143	204	30.85	122	185	35.36	135	199	30.35
128	183	42.12	122	180	39.05	121	181	36.89	144	205	30.55	123	186	36.33	136	200	30.00
129	184	40.77	123	181	39.94	122	182	37.44	$Z = 62$ (Sm)			124	187	36.90	137	201	29.98
130	185	39.26	124	182	40.59	123	183	38.51	109	171	32.27	125	188	38.37	138	202	29.82
$Z = 56$ (Ba)			125	183	41.89	124	184	39.11	110	172	32.19	126	189	38.73	139	203	29.61
115	171	36.71	126	184	42.24	125	185	40.47	111	173	31.96	127	190	37.75	140	204	29.60
116	172	37.22	127	185	41.23	126	186	40.86	112	174	32.04	128	191	36.78	141	205	29.45
117	173	37.85	128	186	40.17	127	187	39.83	113	175	32.15	129	192	35.84	142	206	29.60
118	174	38.29	129	187	38.83	128	188	38.86	114	176	32.07	130	193	34.82	143	207	29.58
119	175	39.14	130	188	37.53	129	189	37.60	115	177	32.50	131	194	34.65	144	208	29.58
120	176	39.32	131	189	36.93	130	190	36.51	116	178	32.59	132	195	33.47	145	209	29.50
121	177	40.20	132	190	36.19	131	191	35.97	117	179	33.13	133	196	32.85	146	210	29.12

TABLE I. (*Continued.*)

N	A	B_f (MeV)	N	A	B_f (MeV)	N	A	B_f (MeV)	N	A	B_f (MeV)	N	A	B_f (MeV)	N	A	B_f (MeV)
$Z = 64$ (Gd)			$Z = 66$ (Dy)			$Z = 67$ (Ho)			$Z = 68$ (Er)			$Z = 69$ (Tm)			$Z = 70$ (Yb)		
147	211	29.00	107	173	32.35	110	177	31.30	110	178	30.10	107	176	30.87	101	171	28.60
148	212	28.75	108	174	32.39	111	178	30.91	111	179	29.80	108	177	30.40	102	172	29.20
149	213	28.85	109	175	31.98	112	179	30.42	112	180	29.36	109	178	30.17	103	173	29.89
150	214	28.69	110	176	31.55	113	180	30.36	113	181	29.60	110	179	30.01	104	174	29.84
$Z = 65$ (Tb)			111	177	31.19	114	181	30.28	114	182	29.88	111	180	29.54	105	175	30.22
106	171	33.01	112	178	30.85	115	182	30.61	115	183	29.85	112	181	29.04	106	176	30.19
107	172	32.80	113	179	30.65	116	183	30.55	116	184	30.04	113	182	29.03	107	177	30.47
108	173	32.60	114	180	30.60	117	184	31.09	117	185	30.28	114	183	29.02	108	178	30.35
109	174	32.17	115	181	31.05	118	185	31.04	118	186	30.44	115	184	29.05	109	179	30.07
110	175	31.84	116	182	31.01	119	186	31.43	119	187	30.90	116	185	29.16	110	180	29.82
111	176	31.41	117	183	31.43	120	187	31.81	120	188	31.35	117	186	29.34	111	181	29.45
112	177	30.95	118	184	31.58	121	188	32.43	121	189	31.74	118	187	29.55	112	182	28.91
113	178	30.99	119	185	31.99	122	189	32.56	122	190	31.80	119	188	30.00	113	183	28.54
114	179	30.91	120	186	32.39	123	190	33.44	123	191	32.55	120	189	30.75	114	184	28.44
115	180	31.31	121	187	32.99	124	191	33.68	124	192	32.98	121	190	31.09	115	185	28.48
116	181	31.43	122	188	33.15	125	192	34.82	125	193	34.15	122	191	31.18	116	186	28.34
117	182	31.92	123	189	33.86	126	193	35.31	126	194	34.51	123	192	31.93	117	187	28.55
118	183	32.08	124	190	34.37	127	194	34.28	127	195	33.46	124	193	32.45	118	188	28.71
119	184	32.51	125	191	35.51	128	195	33.32	128	196	32.72	125	194	33.61	119	189	29.08
120	185	32.94	126	192	36.05	129	196	32.30	129	197	31.55	126	195	34.02	120	190	29.91
121	186	33.67	127	193	34.88	130	197	31.22	130	198	30.32	127	196	32.84	121	191	30.48
122	187	33.93	128	194	34.06	131	198	30.66	131	199	29.56	128	197	32.02	122	192	30.70
123	188	34.78	129	195	33.15	132	199	29.73	132	200	28.59	129	198	30.82	123	193	31.42
124	189	35.25	130	196	32.08	133	200	29.29	133	201	28.07	130	199	29.50	124	194	31.94
125	190	36.39	131	197	31.55	134	201	28.56	134	202	27.42	131	200	28.76	125	195	32.93
126	191	36.97	132	198	30.57	135	202	28.43	135	203	27.23	132	201	27.86	126	196	33.36
127	192	35.86	133	199	29.99	136	203	28.19	136	204	27.05	133	202	27.41	127	197	32.30
128	193	34.90	134	200	29.22	137	204	28.44	137	205	27.23	134	203	26.74	128	198	31.37
129	194	34.12	135	201	28.88	138	205	28.23	138	206	27.04	135	204	26.59	129	199	29.98
130	195	32.99	136	202	28.60	139	206	28.58	139	207	27.31	136	205	26.35	130	200	28.77
131	196	32.72	137	203	28.79	140	207	28.41	140	208	27.25	137	206	26.57	131	201	27.70
132	197	31.76	138	204	28.64	141	208	28.26	141	209	27.21	138	207	26.47	132	202	26.78
133	198	31.19	139	205	28.55	142	209	28.25	142	210	27.24	139	208	26.78	133	203	26.22
134	199	30.32	140	206	28.46	143	210	28.47	143	211	27.29	140	209	26.59	134	204	25.69
135	200	29.99	141	207	28.43	144	211	28.47	144	212	27.42	141	210	27.07	135	205	25.39
136	201	29.63	142	208	28.47	145	212	28.56	145	213	27.50	142	211	26.98	136	206	25.16
137	202	29.83	143	209	28.65	146	213	28.43	146	214	27.55	143	212	27.07	137	207	25.26
138	203	29.60	144	210	28.65	147	214	28.19	147	215	27.31	144	213	27.14	138	208	25.20
139	204	29.55	145	211	28.73	148	215	28.10	148	216	27.19	145	214	27.19	139	209	25.55
140	205	29.49	146	212	28.54	149	216	28.10	149	217	27.23	146	215	27.33	140	210	25.29
141	206	29.40	147	213	28.27	150	217	28.04	150	218	27.20	147	216	27.15	141	211	25.67
142	207	29.45	148	214	28.20	151	218	27.99	151	219	27.08	148	217	26.96	142	212	25.67
143	208	29.60	149	215	28.21	152	219	27.53	152	220	26.76	149	218	27.04	143	213	25.77
144	209	29.55	150	216	28.13	153	220	27.26	153	221	26.49	150	219	26.88	144	214	25.88
145	210	29.57	151	217	28.02	154	221	26.79	154	222	26.14	151	220	26.84	145	215	25.93
146	211	29.16	152	218	27.62	155	222	26.52	155	223	26.00	152	221	26.50	146	216	26.08
147	212	29.07	153	219	27.28	156	223	26.09	156	224	25.64	153	222	26.38	147	217	26.04
148	213	28.69	154	220	26.84	157	224	25.73	157	225	25.34	154	223	26.05	148	218	25.86
149	214	28.98	155	221	26.53	$Z = 68$ (Er)			158	226	24.80	155	224	25.93	149	219	26.04
150	215	28.72	$Z = 67$ (Ho)			103	171	32.34	159	227	24.50	156	225	25.57	150	220	25.87
151	216	28.62	104	171	31.25	104	172	31.21	$Z = 69$ (Tm)			157	226	25.41	151	221	25.89
152	217	28.31	105	172	31.49	105	173	31.27	102	171	30.81	158	227	24.78	152	222	25.68
153	218	27.84	106	173	31.15	106	174	31.02	103	172	31.28	159	228	24.64	153	223	25.53
$Z = 66$ (Dy)			107	174	31.57	107	175	30.51	104	173	31.02	160	229	24.19	154	224	25.32
105	171	32.57	108	175	31.40	108	176	30.37	105	174	31.35	161	230	24.02	155	225	25.19
106	172	31.84	109	176	31.71	109	177	30.27	106	175	31.09				156	226	24.80

TABLE I. (*Continued.*)

N	A	B_f (MeV)	N	A	B_f (MeV)	N	A	B_f (MeV)	N	A	B_f (MeV)	N	A	B_f (MeV)	N	A	B_f (MeV)
$Z = 70$ (Yb)			$Z = 71$ (Lu)			$Z = 72$ (Hf)			$Z = 73$ (Ta)			$Z = 74$ (W)			$Z = 74$ (W)		
157	227	24.64	147	218	25.69	134	206	23.93	118	191	27.09	99	173	20.71	155	229	22.47
158	228	24.12	148	219	25.51	135	207	23.53	119	192	27.48	100	174	21.16	156	230	22.08
159	229	24.02	149	220	25.68	136	208	23.12	120	193	27.79	101	175	21.80	157	231	21.99
160	230	23.66	150	221	25.50	137	209	23.08	121	194	28.70	102	176	22.25	158	232	21.60
161	231	23.58	151	222	25.63	138	210	22.90	122	195	29.03	103	177	22.97	159	233	21.69
162	232	23.32	152	223	25.49	139	211	23.31	123	196	29.80	104	178	23.47	160	234	21.49
163	233	23.07	153	224	25.35	140	212	23.25	124	197	30.19	105	179	24.14	161	235	21.49
164	234	22.38	154	225	25.09	141	213	23.71	125	198	31.07	106	180	24.57	162	236	21.49
$Z = 71$ (Lu)			155	226	25.03	142	214	23.71	126	199	31.35	107	181	25.13	163	237	21.27
100	171	26.54	156	227	24.59	143	215	24.22	127	200	30.55	108	182	25.26	164	238	20.96
101	172	27.28	157	228	24.50	144	216	24.07	128	201	29.64	109	183	25.58	165	239	20.80
102	173	27.65	158	229	23.95	145	217	24.25	129	202	28.48	110	184	25.44	166	240	20.27
103	174	28.42	159	230	23.94	146	218	24.23	130	203	27.06	111	185	25.71	167	241	20.19
104	175	28.92	160	231	23.60	147	219	24.43	131	204	25.86	112	186	25.85	168	242	19.66
105	176	29.42	161	232	23.60	148	220	24.29	132	205	24.55	113	187	26.36	169	243	19.56
106	177	29.54	162	233	23.37	149	221	24.49	133	206	23.91	114	188	26.71	170	244	19.17
107	178	29.86	163	234	23.18	150	222	24.41	134	207	23.28	115	189	26.40	171	245	19.23
108	179	29.92	164	235	22.44	151	223	24.46	135	208	23.13	116	190	26.43	172	246	18.74
109	180	29.89	165	236	22.02	152	224	24.44	136	209	22.60	117	191	26.55	173	247	18.59
110	181	29.50	166	237	21.35	153	225	24.30	137	210	22.75	118	192	26.86	$Z = 75$ (Re)		
111	182	29.25	$Z = 72$ (Hf)			154	226	24.11	138	211	22.70	119	193	27.01	96	171	17.51
112	183	28.62	99	171	24.26	155	227	24.08	139	212	22.51	120	194	27.44	97	172	17.94
113	184	28.23	100	172	24.65	156	228	23.65	140	213	22.78	121	195	27.99	98	173	18.13
114	185	28.00	101	173	25.30	157	229	23.56	141	214	23.19	122	196	28.45	99	174	18.81
115	186	27.90	102	174	25.84	158	230	23.18	142	215	23.24	123	197	29.18	100	175	19.23
116	187	27.68	103	175	26.52	159	231	23.09	143	216	23.69	124	198	29.63	101	176	19.95
117	188	28.00	104	176	27.09	160	232	22.83	144	217	23.46	125	199	30.69	102	177	20.56
118	189	28.26	105	177	27.59	161	233	22.81	145	218	23.65	126	200	30.96	103	178	21.38
119	190	28.44	106	178	28.21	162	234	22.66	146	219	23.71	127	201	30.05	104	179	21.82
120	191	29.43	107	179	28.92	163	235	22.39	147	220	23.92	128	202	29.28	105	180	22.50
121	192	29.91	108	180	28.72	164	236	22.03	148	221	23.78	129	203	28.08	106	181	22.91
122	193	30.09	109	181	28.93	165	237	21.57	149	222	23.90	130	204	26.83	107	182	23.49
123	194	30.82	110	182	28.65	166	238	20.94	150	223	23.90	131	205	25.26	108	183	23.62
124	195	31.26	111	183	28.75	167	239	20.74	151	224	24.02	132	206	24.09	109	184	23.77
125	196	32.25	112	184	28.07	168	240	20.04	152	225	23.98	133	207	23.14	110	185	23.66
126	197	32.57	113	185	27.64	$Z = 73$ (Ta)			153	226	23.94	134	208	22.79	111	186	24.13
127	198	31.67	114	186	27.24	98	171	21.96	154	227	23.69	135	209	22.42	112	187	24.12
128	199	30.75	115	187	26.98	99	172	22.76	155	228	23.64	136	210	21.83	113	188	24.77
129	200	29.36	116	188	26.90	100	173	23.14	156	229	23.26	137	211	21.95	114	189	25.13
130	201	28.10	117	189	27.01	101	174	23.93	157	230	23.20	138	212	21.77	115	190	25.99
131	202	26.98	118	190	27.44	102	175	24.41	158	231	22.75	139	213	21.83	116	191	26.24
132	203	26.05	119	191	27.71	103	176	25.17	159	232	22.83	140	214	21.61	117	192	26.37
133	204	25.53	120	192	28.61	104	177	25.42	160	233	22.53	141	215	22.07	118	193	26.57
134	205	24.99	121	193	29.30	105	178	26.20	161	234	22.59	142	216	22.08	119	194	26.64
135	206	24.73	122	194	29.61	106	179	26.62	162	235	22.46	143	217	22.49	120	195	26.76
136	207	24.36	123	195	30.32	107	180	27.26	163	236	22.27	144	218	22.27	121	196	27.44
137	208	24.53	124	196	30.80	108	181	27.37	164	237	21.91	145	219	22.16	122	197	27.93
138	209	24.35	125	197	31.65	109	182	27.58	165	238	21.55	146	220	22.40	123	198	28.69
139	210	24.62	126	198	32.03	110	183	27.62	166	239	20.94	147	221	22.46	124	199	29.07
140	211	24.58	127	199	31.12	111	184	28.00	167	240	20.77	148	222	22.44	125	200	29.91
141	212	25.11	128	200	30.19	112	185	27.79	168	241	20.12	149	223	22.53	126	201	30.22
142	213	25.05	129	201	28.93	113	186	27.72	169	242	19.95	150	224	22.64	127	202	29.48
143	214	25.44	130	202	27.70	114	187	27.14	170	243	19.48	151	225	22.68	128	203	28.54
144	215	25.46	131	203	26.17	115	188	26.84	$Z = 74$ (W)			152	226	22.71	129	204	27.39
145	216	25.63	132	204	25.03	116	189	26.66	97	171	19.82	153	227	22.66	130	205	26.18
146	217	25.63	133	205	24.44	117	190	26.91	98	172	20.03	154	228	22.45	131	206	25.13

TABLE I. (*Continued.*)

N	A	B_f (MeV)	N	A	B_f (MeV)	N	A	B_f (MeV)	N	A	B_f (MeV)	N	A	B_f (MeV)	N	A	B_f (MeV)
$Z = 75$ **(Re)**			$Z = 76$ **(Os)**			$Z = 76$ **(Os)**			$Z = 77$ **(Lr)**			$Z = 78$ **(Pt)**			$Z = 78$ **(Pt)**		
132	207	23.73	106	182	20.76	162	238	19.97	133	210	21.98	101	179	13.34	157	235	17.54
133	208	22.96	107	183	21.20	163	239	19.78	134	211	21.45	102	180	13.78	158	236	17.24
134	209	22.37	108	184	21.29	164	240	19.21	135	212	21.13	103	181	14.43	159	237	17.18
135	210	22.22	109	185	21.41	165	241	19.22	136	213	20.75	104	182	14.90	160	238	17.33
136	211	21.72	110	186	21.44	166	242	18.75	137	214	20.50	105	183	15.46	161	239	17.49
137	212	21.67	111	187	21.67	167	243	18.78	138	215	19.99	106	184	16.09	162	240	17.63
138	213	21.62	112	188	21.75	168	244	18.53	139	216	19.49	107	185	16.66	163	241	17.56
139	214	21.68	113	189	22.38	169	245	18.61	140	217	18.91	108	186	17.06	164	242	17.18
140	215	21.18	114	190	22.89	170	246	18.47	141	218	18.58	109	187	17.59	165	243	16.97
141	216	21.37	115	191	23.85	171	247	18.68	142	219	18.31	110	188	17.75	166	244	16.82
142	217	21.09	116	192	24.84	172	248	18.28	143	220	18.46	111	189	18.26	167	245	16.80
143	218	21.36	117	193	25.33	173	249	18.17	144	221	18.27	112	190	18.80	168	246	16.70
144	219	21.33	118	194	25.58	174	250	17.78	145	222	18.57	113	191	19.60	169	247	17.00
145	220	21.43	119	195	25.84	175	251	17.26	146	223	18.62	114	192	20.08	170	248	16.86
146	221	21.74	120	196	26.15	176	252	17.37	147	224	18.99	115	193	20.84	171	249	17.30
147	222	21.91	121	197	26.75	177	253	18.11	148	225	19.08	116	194	21.47	172	250	17.33
148	223	22.00	122	198	27.29	$Z = 77$ **(Ir)**			149	226	19.48	117	195	22.26	173	251	17.54
149	224	22.00	123	199	28.07	94	171	13.83	150	227	19.49	118	196	23.01	174	252	17.33
150	225	22.06	124	200	28.54	95	172	14.18	151	228	19.83	119	197	23.67	175	253	17.54
151	226	22.09	125	201	29.55	96	173	13.98	152	229	19.46	120	198	24.54	176	254	17.49
152	227	22.11	126	202	29.83	97	174	14.11	153	230	19.44	121	199	25.52	177	255	17.77
153	228	22.13	127	203	29.07	98	175	14.14	154	231	18.76	122	200	26.30	178	256	17.75
154	229	21.68	128	204	28.21	99	176	14.66	155	232	18.97	123	201	27.06	179	257	17.89
155	230	21.65	129	205	27.08	100	177	14.77	156	233	18.88	124	202	27.51	180	258	17.65
156	231	21.35	130	206	25.98	101	178	15.47	157	234	19.17	125	203	28.34	181	259	17.70
157	232	21.47	131	207	24.67	102	179	16.03	158	235	18.79	126	204	28.50	182	260	17.33
158	233	21.12	132	208	23.29	103	180	16.65	159	236	18.67	127	205	27.64	$Z = 79$ **(Au)**		
159	234	21.24	133	209	22.24	104	181	17.26	160	237	18.67	128	206	26.98	92	171	10.83
160	235	20.93	134	210	21.74	105	182	17.82	161	238	18.93	129	207	25.77	93	172	10.94
161	236	21.05	135	211	21.53	106	183	18.30	162	239	19.09	130	208	24.77	94	173	10.94
162	237	21.02	136	212	21.04	107	184	18.84	163	240	18.93	131	209	23.44	95	174	10.64
163	238	20.94	137	213	20.80	108	185	18.98	164	241	18.49	132	210	22.33	96	175	11.00
164	239	20.62	138	214	20.46	109	186	19.53	165	242	18.42	133	211	21.48	97	176	11.28
165	240	20.44	139	215	20.41	110	187	19.59	166	243	17.94	134	212	20.81	98	177	11.07
166	241	19.98	140	216	20.12	111	188	20.06	167	244	18.12	135	213	20.32	99	178	11.23
167	242	19.94	141	217	19.75	112	189	20.15	168	245	18.04	136	214	19.74	100	179	11.36
168	243	19.41	142	218	19.50	113	190	20.69	169	246	18.16	137	215	19.44	101	180	11.83
169	244	19.42	143	219	19.57	114	191	20.94	170	247	17.94	138	216	18.97	102	181	12.28
170	245	19.12	144	220	19.57	115	192	22.19	171	248	18.50	139	217	18.35	103	182	12.76
171	246	19.28	145	221	19.84	116	193	23.18	172	249	18.17	140	218	17.75	104	183	13.20
172	247	18.75	146	222	19.90	117	194	23.84	173	250	18.03	141	219	17.32	105	184	13.84
173	248	18.68	147	223	20.25	118	195	24.31	174	251	17.57	142	220	16.90	106	185	14.31
174	249	18.16	148	224	20.41	119	196	24.95	175	252	17.73	143	221	16.70	107	186	15.03
175	250	17.93	149	225	20.50	120	197	25.27	176	253	17.45	144	222	16.67	108	187	15.33
$Z = 76$ **(Os)**			150	226	20.66	121	198	26.22	177	254	18.25	145	223	16.70	109	188	16.01
95	171	15.38	151	227	20.67	122	199	26.92	178	255	18.03	146	224	16.78	110	189	16.57
96	172	15.49	152	228	20.66	123	200	27.70	179	256	18.17	147	225	16.98	111	190	17.16
97	173	15.87	153	229	20.39	124	201	28.18	$Z = 78$ **(Pt)**			148	226	17.08	112	191	17.99
98	174	16.01	154	230	19.94	125	202	29.05	93	171	11.36	149	227	17.55	113	192	18.87
99	175	16.37	155	231	19.94	126	203	29.35	94	172	11.73	150	228	17.45	114	193	19.26
100	176	16.97	156	232	19.79	127	204	28.46	95	173	12.23	151	229	17.75	115	194	19.96
101	177	17.58	157	233	20.14	128	205	27.77	96	174	12.39	152	230	17.65	116	195	20.54
102	178	18.12	158	234	19.80	129	206	26.69	97	175	12.52	153	231	17.33	117	196	21.47
103	179	18.79	159	235	19.70	130	207	25.59	98	176	12.38	154	232	17.22	118	197	22.31
104	180	19.49	160	236	19.62	131	208	24.27	99	177	12.48	155	233	17.47	119	198	23.16
105	181	20.17	161	237	19.79	132	209	22.95	100	178	12.82	156	234	17.42	120	199	23.97

TABLE I. (*Continued.*)

N	A	B_f (MeV)	N	A	B_f (MeV)	N	A	B_f (MeV)	N	A	B_f (MeV)	N	A	B_f (MeV)	N	A	B_f (MeV)
$Z = 79$ (Au)			$Z = 79$ (Au)			$Z = 80$ (Hg)			$Z = 81$ (Tl)			$Z = 81$ (Tl)			$Z = 82$ (Pb)		
121	200	25.07	177	256	17.64	138	218	17.04	98	179	8.81	154	235	13.81	113	195	14.77
122	201	25.78	178	257	17.61	139	219	16.53	99	180	8.65	155	236	13.94	114	196	15.66
123	202	26.53	179	258	17.86	140	220	15.69	100	181	8.86	156	237	13.78	115	197	16.36
124	203	27.01	180	259	17.60	141	221	15.13	101	182	8.98	157	238	14.12	116	198	17.28
125	204	27.95	181	260	17.61	142	222	14.56	102	183	9.49	158	239	14.02	117	199	18.09
126	205	28.03	182	261	17.31	143	223	14.41	103	184	9.87	159	240	14.29	118	200	18.89
127	206	27.09	183	262	17.32	144	224	14.13	104	185	10.44	160	241	14.07	119	201	19.67
128	207	26.36	184	263	17.27	145	225	14.19	105	186	10.97	161	242	14.31	120	202	20.48
129	208	25.36	$Z = 80$ (Hg)			146	226	14.30	106	187	11.48	162	243	14.37	121	203	20.91
130	209	24.25	91	171	10.03	147	227	14.59	107	188	12.11	163	244	14.43	122	204	21.91
131	210	22.93	92	172	9.81	148	228	14.71	108	189	12.74	164	245	14.19	123	205	23.08
132	211	21.87	93	173	9.79	149	229	15.09	109	190	13.49	165	246	14.35	124	206	23.94
133	212	21.29	94	174	9.63	150	230	14.95	110	191	14.31	166	247	14.53	125	207	24.76
134	213	20.54	95	175	9.77	151	231	15.16	111	192	15.13	167	248	14.88	126	208	24.95
135	214	19.95	96	176	9.62	152	232	14.97	112	193	15.99	168	249	15.23	127	209	23.97
136	215	19.25	97	177	9.41	153	233	15.11	113	194	16.38	169	250	15.62	128	210	22.91
137	216	18.84	98	178	9.32	154	234	14.85	114	195	17.08	170	251	15.98	129	211	21.88
138	217	18.24	99	179	9.68	155	235	15.09	115	196	18.04	171	252	16.53	130	212	20.77
139	218	17.77	100	180	9.81	156	236	14.97	116	197	18.85	172	253	16.75	131	213	19.87
140	219	16.95	101	181	10.27	157	237	14.99	117	198	19.73	173	254	17.20	132	214	19.13
141	220	16.41	102	182	10.85	158	238	14.91	118	199	20.63	174	255	17.10	133	215	18.43
142	221	15.77	103	183	11.32	159	239	14.90	119	200	21.66	175	256	17.50	134	216	17.95
143	222	15.58	104	184	11.92	160	240	14.97	120	201	22.23	176	257	17.58	135	217	17.48
144	223	15.51	105	185	12.43	161	241	15.21	121	202	23.29	177	258	17.76	136	218	16.83
145	224	15.44	106	186	12.99	162	242	15.24	122	203	24.04	178	259	17.90	137	219	16.13
146	225	15.35	107	187	13.50	163	243	15.22	123	204	24.80	179	260	18.33	138	220	15.33
147	226	15.71	108	188	13.98	164	244	14.90	124	205	25.49	180	261	18.18	139	221	14.45
148	227	15.79	109	189	14.52	165	245	14.71	125	206	26.38	181	262	18.51	140	222	13.70
149	228	16.52	110	190	15.22	166	246	15.11	126	207	26.50	182	263	18.25	141	223	12.89
150	229	16.18	111	191	16.02	167	247	15.50	127	208	25.55	183	264	18.37	142	224	12.48
151	230	16.98	112	192	16.75	168	248	15.77	128	209	24.72	184	265	17.79	143	225	12.43
152	231	16.31	113	193	17.56	169	249	16.12	129	210	23.55	185	266	16.95	144	226	12.34
153	232	16.48	114	194	18.10	170	250	16.40	130	211	22.42	186	267	15.93	145	227	12.30
154	233	16.25	115	195	18.79	171	251	16.79	131	212	21.58	187	268	14.45	146	228	12.16
155	234	16.50	116	196	19.65	172	252	16.89	132	213	20.79	188	269	13.28	147	229	12.39
156	235	16.36	117	197	20.48	173	253	17.28	133	214	19.97	$Z = 82$ (Pb)			148	230	12.58
157	236	16.46	118	198	21.45	174	254	17.38	134	215	19.19	93	175	7.62	149	231	12.82
158	237	16.23	119	199	22.24	175	255	17.74	135	216	18.50	94	176	7.58	150	232	12.67
159	238	16.41	120	200	23.23	176	256	17.62	136	217	17.78	95	177	7.74	151	233	12.90
160	239	16.47	121	201	24.05	177	257	17.77	137	218	17.31	96	178	7.99	152	234	12.64
161	240	16.58	122	202	24.79	178	258	17.76	138	219	16.50	97	179	8.15	153	235	12.70
162	241	16.63	123	203	25.55	179	259	18.02	139	220	15.88	98	180	8.47	154	236	12.41
163	242	16.61	124	204	26.11	180	260	17.79	140	221	14.99	99	181	8.48	155	237	12.40
164	243	16.24	125	205	27.09	181	261	17.84	141	222	14.33	100	182	8.62	156	238	12.23
165	244	16.08	126	206	27.21	182	262	17.69	142	223	13.64	101	183	8.65	157	239	12.37
166	245	15.69	127	207	26.10	183	263	17.75	143	224	13.49	102	184	8.92	158	240	12.42
167	246	15.99	128	208	25.51	184	264	17.41	144	225	13.33	103	185	9.12	159	241	12.81
168	247	16.24	129	209	24.37	185	265	16.52	145	226	13.54	104	186	9.61	160	242	12.77
169	248	16.77	130	210	23.32	186	266	15.63	146	227	13.53	105	187	9.83	161	243	13.01
170	249	16.94	131	211	22.17	$Z = 81$ (Tl)			147	228	13.89	106	188	10.32	162	244	13.07
171	250	17.57	132	212	21.27	92	173	9.11	148	229	13.86	107	189	10.63	163	245	13.21
172	251	17.57	133	213	20.44	93	174	8.96	149	230	14.15	108	190	11.18	164	246	13.24
173	252	17.82	134	214	19.80	94	175	9.13	150	231	13.99	109	191	11.68	165	247	13.42
174	253	17.39	135	215	19.00	95	176	9.19	151	232	14.20	110	192	12.85	166	248	13.60
175	254	17.70	136	216	18.33	96	177	9.04	152	233	13.96	111	193	13.57	167	249	13.85
176	255	17.77	137	217	17.73	97	178	9.01	153	234	14.09	112	194	14.50	168	250	14.06

TABLE I. (*Continued.*)

N	A	B_f (MeV)	N	A	B_f (MeV)	N	A	B_f (MeV)	N	A	B_f (MeV)	N	A	B_f (MeV)	N	A	B_f (MeV)
$Z = 82$ (Pb)			$Z = 83$ (Bi)			$Z = 83$ (Bi)			$Z = 84$ (Po)			$Z = 85$ (At)			$Z = 85$ (At)		
169	251	14.61	127	210	22.74	183	266	17.52	141	225	11.24	99	184	4.12	155	240	9.79
170	252	14.85	128	211	21.76	184	267	16.96	142	226	10.98	100	185	4.39	156	241	9.58
171	253	15.29	129	212	20.49	185	268	15.81	143	227	10.92	101	186	4.68	157	242	9.94
172	254	15.28	130	213	19.17	186	269	14.74	144	228	10.68	102	187	5.00	158	243	9.73
173	255	15.72	131	214	17.89	187	270	13.30	145	229	10.66	103	188	5.44	159	244	10.19
174	256	15.67	132	215	16.79	188	271	11.66	146	230	10.63	104	189	5.56	160	245	10.17
175	257	16.18	133	216	16.05	189	272	11.88	147	231	10.75	105	190	5.94	161	246	10.41
176	258	16.30	134	217	15.65	190	273	11.25	148	232	10.69	106	191	6.02	162	247	10.42
177	259	17.03	135	218	15.16	191	274	11.23	149	233	10.97	107	192	6.76	163	248	10.60
178	260	17.33	136	219	14.45	192	275	10.76	150	234	10.76	108	193	7.24	164	249	10.49
179	261	17.87	137	220	14.02	193	276	9.86	151	235	11.08	109	194	7.67	165	250	10.75
180	262	17.97	138	221	13.33	$Z = 84$ (Po)			152	236	10.83	110	195	7.96	166	251	10.88
181	263	18.30	139	222	12.58	97	181	3.89	153	237	10.85	111	196	8.33	167	252	11.26
182	264	18.08	140	223	12.26	98	182	4.35	154	238	10.49	112	197	8.63	168	253	11.47
183	265	18.20	141	224	12.31	99	183	4.89	155	239	10.49	113	198	9.10	169	254	12.04
184	266	17.71	142	225	12.14	100	184	5.49	156	240	10.11	114	199	9.95	170	255	12.22
185	267	16.50	143	226	11.92	101	185	5.93	157	241	10.28	115	200	10.80	171	256	12.53
186	268	15.43	144	227	11.79	102	186	6.35	158	242	10.34	116	201	11.73	172	257	13.04
187	269	13.94	145	228	11.71	103	187	6.64	159	243	10.62	117	202	12.66	173	258	12.82
188	270	12.96	146	229	11.66	104	188	6.92	160	244	10.61	118	203	13.70	174	259	12.94
189	271	12.57	147	230	11.77	105	189	7.27	161	245	10.99	119	204	14.72	175	260	13.24
190	272	12.09	148	231	11.44	106	190	7.55	162	246	10.95	120	205	15.41	176	261	13.65
191	273	11.96	149	232	11.84	107	191	7.89	163	247	11.42	121	206	16.63	177	262	14.18
$Z = 83$ (Bi)			150	233	11.65	108	192	8.25	164	248	11.35	122	207	17.46	178	263	14.37
95	178	5.33	151	234	11.87	109	193	8.66	165	249	11.56	123	208	18.31	179	264	14.66
96	179	5.40	152	235	11.56	110	194	9.46	166	250	11.69	124	209	19.10	180	265	14.81
97	180	5.69	153	236	11.56	111	195	9.59	167	251	12.04	125	210	19.99	181	266	15.21
98	181	5.73	154	237	11.36	112	196	10.29	168	252	12.29	126	211	20.27	182	267	15.13
99	182	6.40	155	238	11.14	113	197	10.66	169	253	12.83	127	212	19.37	183	268	15.30
100	183	6.53	156	239	10.96	114	198	11.52	170	254	12.98	128	213	18.56	184	269	14.82
101	184	7.16	157	240	11.28	115	199	12.37	171	255	13.35	129	214	17.35	185	270	13.70
102	185	7.38	158	241	11.29	116	200	13.31	172	256	13.73	130	215	16.03	186	271	12.88
103	186	7.75	159	242	11.55	117	201	14.18	173	257	13.69	131	216	14.99	187	272	11.34
104	187	7.75	160	243	11.44	118	202	15.14	174	258	13.70	132	217	14.16	188	273	10.89
105	188	8.14	161	244	11.68	119	203	16.15	175	259	14.20	133	218	13.31	189	274	10.46
106	189	8.60	162	245	11.72	120	204	17.02	176	260	14.61	134	219	12.46	190	275	10.14
107	190	9.15	163	246	12.08	121	205	18.08	177	261	15.12	135	220	12.12	191	276	10.05
108	191	9.45	164	247	11.97	122	206	19.02	178	262	15.24	136	221	11.75	192	277	9.12
109	192	9.99	165	248	12.66	123	207	20.01	179	263	15.83	137	222	11.64	193	278	8.69
110	193	10.59	166	249	12.78	124	208	20.81	180	264	16.02	138	223	11.13	194	279	7.97
111	194	11.14	167	250	13.10	125	209	22.24	181	265	16.41	139	224	11.03	195	280	7.13
112	195	11.79	168	251	13.46	126	210	22.14	182	266	16.33	140	225	10.74	196	281	6.46
113	196	12.31	169	252	14.06	127	211	21.33	183	267	16.51	141	226	10.42	197	282	6.20
114	197	13.29	170	253	14.25	128	212	20.27	184	268	16.05	142	227	10.11	$Z = 86$ (Rn)		
115	198	14.23	171	254	14.59	129	213	18.99	185	269	14.82	143	228	10.02	100	186	4.19
116	199	15.22	172	255	14.74	130	214	17.76	186	270	13.86	144	229	9.83	101	187	4.43
117	200	16.18	173	256	14.94	131	215	16.47	187	271	12.36	145	230	9.86	102	188	4.45
118	201	16.99	174	257	14.81	132	216	15.42	188	272	11.82	146	231	9.78	103	189	4.62
119	202	17.90	175	258	15.42	133	217	14.56	189	273	11.49	147	232	9.97	104	190	4.54
120	203	18.71	176	259	15.81	134	218	13.85	190	274	10.85	148	233	9.93	105	191	4.49
121	204	19.59	177	260	16.27	135	219	12.93	191	275	10.84	149	234	10.18	106	192	4.63
122	205	20.47	178	261	16.42	136	220	12.47	192	276	10.02	150	235	10.36	107	193	5.02
123	206	21.42	179	262	17.06	137	221	12.31	193	277	9.16	151	236	10.60	108	194	5.43
124	207	22.28	180	263	17.19	138	222	11.91	194	278	8.48	152	237	10.53	109	195	6.05
125	208	23.23	181	264	17.59	139	223	11.70	195	279	7.86	153	238	10.31	110	196	6.41
126	209	23.88	182	265	17.41	140	224	11.46				154	239	10.04	111	197	6.83

TABLE I. (*Continued.*)

N	A	B_f (MeV)	N	A	B_f (MeV)	N	A	B_f (MeV)	N	A	B_f (MeV)	N	A	B_f (MeV)	N	A	B_f (MeV)
$Z = 86$ (Rn)			$Z = 86$ (Rn)			$Z = 87$ (Fr)			$Z = 87$ (Fr)			$Z = 88$ (Ra)			$Z = 88$ (Ra)		
112	198	7.40	168	254	10.03	124	211	16.02	180	267	12.32	136	224	8.78	192	280	7.64
113	199	8.09	169	255	10.52	125	212	16.72	181	268	12.65	137	225	8.40	193	281	7.16
114	200	8.61	170	256	10.81	126	213	16.66	182	269	12.79	138	226	8.23	194	282	6.46
115	201	9.39	171	257	11.22	127	214	15.65	183	270	13.05	139	227	8.02	195	283	6.10
116	202	10.29	172	258	11.60	128	215	14.81	184	271	12.54	140	228	7.61	196	284	5.56
117	203	11.16	173	259	11.32	129	216	13.46	185	272	11.55	141	229	7.31	197	285	5.19
118	204	12.10	174	260	11.35	130	217	12.74	186	273	10.76	142	230	7.04	198	286	4.77
119	205	13.20	175	261	11.91	131	218	12.40	187	274	9.74	143	231	7.01	199	287	4.26
120	206	14.20	176	262	12.30	132	219	11.57	188	275	9.09	144	232	6.94	200	288	3.78
121	207	15.14	177	263	12.79	133	220	11.33	189	276	9.18	145	233	6.97	201	289	3.39
122	208	15.94	178	264	12.99	134	221	10.81	190	277	8.93	146	234	6.90	202	290	2.91
123	209	16.75	179	265	13.42	135	222	10.47	191	278	8.72	147	235	7.16	203	291	2.63
124	210	17.61	180	266	13.55	136	223	10.02	192	279	8.17	148	236	7.33	204	292	2.24
125	211	18.47	181	267	13.74	137	224	9.64	193	280	7.72	149	237	7.70	$Z = 89$ (Ac)		
126	212	18.63	182	268	13.81	138	225	9.22	194	281	7.03	150	238	7.79	106	195	3.40
127	213	17.65	183	269	14.07	139	226	9.02	195	282	6.58	151	239	8.26	107	196	3.29
128	214	16.69	184	270	13.59	140	227	8.61	196	283	6.14	152	240	8.24	108	197	3.24
129	215	15.45	185	271	12.54	141	228	8.36	197	284	5.60	153	241	8.24	109	198	3.44
130	216	14.24	186	272	11.68	142	229	8.12	198	285	5.05	154	242	7.95	110	199	3.45
131	217	13.52	187	273	10.71	143	230	8.04	199	286	4.53	155	243	7.78	111	200	3.64
132	218	12.83	188	274	10.02	144	231	7.96	200	287	4.01	156	244	7.49	112	201	4.05
133	219	12.02	189	275	9.74	145	232	8.01	201	288	3.85	157	245	7.61	113	202	4.81
134	220	11.47	190	276	9.42	146	233	7.92	202	289	3.27	158	246	7.34	114	203	5.19
135	221	11.18	191	277	9.22	147	234	8.09	$Z = 88$ (Ra)			159	247	7.39	115	204	5.72
136	222	10.82	192	278	8.45	148	235	8.15	104	192	3.92	160	248	7.20	116	205	6.49
137	223	10.57	193	279	8.04	149	236	8.50	105	193	3.77	161	249	7.29	117	206	7.42
138	224	10.30	194	280	7.37	150	237	8.71	106	194	3.76	162	250	7.21	118	207	8.46
139	225	9.72	195	281	6.62	151	238	8.96	107	195	3.46	163	251	7.26	119	208	9.50
140	226	9.45	196	282	6.09	152	239	9.03	108	196	3.72	164	252	7.08	120	209	10.58
141	227	9.26	197	283	5.45	153	240	9.07	109	197	4.12	165	253	7.14	121	210	11.31
142	228	9.04	198	284	5.13	154	241	8.83	110	198	3.99	166	254	7.10	122	211	12.03
143	229	8.88	199	285	4.43	155	242	8.66	111	199	4.63	167	255	7.33	123	212	12.65
144	230	8.81	200	286	4.00	156	243	8.44	112	200	5.12	168	256	7.48	124	213	12.99
145	231	8.81	$Z = 87$ (Fr)			157	244	8.45	113	201	5.85	169	257	7.75	125	214	13.52
146	232	8.82	102	189	4.24	158	245	8.24	114	202	6.26	170	258	8.07	126	215	13.36
147	233	8.87	103	190	4.44	159	246	8.09	115	203	6.89	171	259	8.52	127	216	12.19
148	234	8.92	104	191	4.33	160	247	8.12	116	204	7.49	172	260	9.00	128	217	11.08
149	235	9.21	105	192	4.43	161	248	8.42	117	205	8.51	173	261	8.87	129	218	10.40
150	236	9.38	106	193	4.38	162	249	8.44	118	206	9.75	174	262	9.03	130	219	10.03
151	237	9.76	107	194	4.35	163	250	8.66	119	207	10.82	175	263	9.73	131	220	9.71
152	238	9.70	108	195	4.48	164	251	8.59	120	208	11.70	176	264	10.16	132	221	9.34
153	239	9.73	109	196	4.58	165	252	8.53	121	209	12.54	177	265	10.73	133	222	9.13
154	240	9.30	110	197	5.18	166	253	8.53	122	210	13.26	178	266	10.80	134	223	8.69
155	241	9.17	111	198	5.82	167	254	8.83	123	211	14.00	179	267	11.18	135	224	8.50
156	242	8.98	112	199	6.39	168	255	9.00	124	212	14.40	180	268	11.15	136	225	8.05
157	243	9.26	113	200	7.10	169	256	9.56	125	213	15.11	181	269	11.68	137	226	7.71
158	244	9.12	114	201	7.62	170	257	9.79	126	214	14.94	182	270	11.74	138	227	7.53
159	245	9.01	115	202	8.33	171	258	10.05	127	215	13.93	183	271	12.02	139	228	7.24
160	246	9.02	116	203	8.92	172	259	10.40	128	216	13.01	184	272	11.58	140	229	6.68
161	247	9.28	117	204	9.64	173	260	10.44	129	217	11.80	185	273	10.53	141	230	6.49
162	248	9.34	118	205	10.94	174	261	10.20	130	218	11.25	186	274	9.78	142	231	6.24
163	249	9.51	119	206	11.98	175	262	10.95	131	219	10.81	187	275	8.88	143	232	6.19
164	250	9.40	120	207	12.85	176	263	11.42	132	220	10.25	188	276	8.33	144	233	6.08
165	251	9.41	121	208	13.71	177	264	11.72	133	221	10.03	189	277	8.48	145	234	6.16
166	252	9.52	122	209	14.60	178	265	11.91	134	222	9.57	190	278	8.22	146	235	6.27
167	253	9.81	123	210	15.40	179	266	12.35	135	223	9.20	191	279	8.20	147	236	6.89

TABLE I. (*Continued.*)

N	A	B_f (MeV)	N	A	B_f (MeV)	N	A	B_f (MeV)	N	A	B_f (MeV)	N	A	B_f (MeV)	N	A	B_f (MeV)
$Z = 89$ (Ac)			$Z = 89$ (Ac)			$Z = 90$ (Th)			$Z = 91$ (Pa)			$Z = 91$ (Pa)			$Z = 92$ (U)		
148	237	7.08	204	293	2.51	160	250	6.59	114	205	3.04	170	261	5.84	124	216	9.25
149	238	7.61	205	294	2.65	161	251	6.63	115	206	4.01	171	262	6.24	125	217	9.78
150	239	7.75	206	295	2.70	162	252	6.40	116	207	4.74	172	263	6.24	126	218	9.67
151	240	8.26	$Z = 90$ (Th)			163	253	6.22	117	208	5.62	173	264	6.30	127	219	8.54
152	241	8.19	108	198	2.53	164	254	6.07	118	209	6.55	174	265	6.33	128	220	7.62
153	242	8.15	109	199	2.77	165	255	5.86	119	210	7.44	175	266	6.82	129	221	7.06
154	243	7.84	110	200	2.69	166	256	5.53	120	211	8.19	176	267	7.14	130	222	6.46
155	244	7.62	111	201	2.89	167	257	5.88	121	212	8.97	177	268	7.59	131	223	5.87
156	245	7.35	112	202	2.86	168	258	6.08	122	213	9.33	178	269	7.93	132	224	5.65
157	246	7.36	113	203	3.61	169	259	6.39	123	214	9.97	179	270	8.46	133	225	5.81
158	247	7.12	114	204	3.85	170	260	6.61	124	215	10.35	180	271	8.49	134	226	5.59
159	248	7.10	115	205	4.79	171	261	7.05	125	216	10.93	181	272	8.98	135	227	5.48
160	249	6.86	116	206	5.44	172	262	7.04	126	217	10.81	182	273	8.91	136	228	5.13
161	250	6.94	117	207	6.43	173	263	6.88	127	218	9.68	183	274	9.13	137	229	4.94
162	251	6.74	118	208	7.57	174	264	7.01	128	219	8.60	184	275	8.65	138	230	4.28
163	252	6.81	119	209	8.55	175	265	7.60	129	220	8.20	185	276	7.57	139	231	4.46
164	253	6.59	120	210	9.39	176	266	8.00	130	221	7.55	186	277	7.09	140	232	4.72
165	254	6.50	121	211	10.11	177	267	8.52	131	222	6.93	187	278	6.41	141	233	4.79
166	255	6.27	122	212	10.66	178	268	8.73	132	223	6.91	188	279	6.23	142	234	4.89
167	256	6.64	123	213	11.34	179	269	9.33	133	224	7.03	189	280	6.35	143	235	4.87
168	257	6.91	124	214	11.68	180	270	9.38	134	225	6.84	190	281	6.20	144	236	5.03
169	258	7.31	125	215	12.34	181	271	9.84	135	226	6.91	191	282	6.31	145	237	5.43
170	259	7.48	126	216	12.17	182	272	9.87	136	227	6.51	192	283	6.01	146	238	5.63
171	260	7.85	127	217	11.02	183	273	10.09	137	228	6.26	193	284	6.11	147	239	6.21
172	261	8.01	128	218	9.99	184	274	9.65	138	229	5.59	194	285	5.93	148	240	6.38
173	262	7.97	129	219	9.17	185	275	8.66	139	230	5.28	195	286	5.85	149	241	6.93
174	263	8.11	130	220	8.45	186	276	8.08	140	231	4.99	196	287	5.46	150	242	7.10
175	264	8.77	131	221	8.27	187	277	7.27	141	232	4.97	197	288	5.23	151	243	7.50
176	265	9.20	132	222	7.99	188	278	6.84	142	233	4.99	198	289	4.76	152	244	7.46
177	266	9.78	133	223	8.20	189	279	7.06	143	234	5.13	199	290	4.30	153	245	7.39
178	267	9.77	134	224	7.85	190	280	6.90	144	235	5.33	200	291	3.85	154	246	7.21
179	268	10.24	135	225	7.59	191	281	6.97	145	236	5.76	201	292	3.60	155	247	7.03
180	269	10.27	136	226	7.20	192	282	6.66	146	237	5.99	202	293	3.11	156	248	6.64
181	270	10.81	137	227	6.98	193	283	6.31	147	238	6.57	203	294	2.98	157	249	6.57
182	271	10.79	138	228	6.52	194	284	5.87	148	239	6.72	204	295	2.83	158	250	6.31
183	272	11.06	139	229	6.06	195	285	5.76	149	240	7.27	205	296	2.99	159	251	6.37
184	273	10.58	140	230	5.66	196	286	5.40	150	241	7.43	206	297	3.07	160	252	6.04
185	274	9.60	141	231	5.55	197	287	5.14	151	242	7.87	207	298	3.34	161	253	6.00
186	275	8.99	142	232	5.44	198	288	4.74	152	243	7.79	208	299	3.32	162	254	5.74
187	276	8.10	143	233	5.47	199	289	4.22	153	244	7.76	209	300	3.39	163	255	5.48
188	277	7.55	144	234	5.38	200	290	3.62	154	245	7.40	210	301	3.17	164	256	5.02
189	278	7.79	145	235	5.80	201	291	3.33	155	246	7.12	211	302	3.06	165	257	4.78
190	279	7.60	146	236	6.04	202	292	3.05	156	247	6.89	$Z = 92$ (U)			166	258	4.61
191	280	7.64	147	237	6.64	203	293	2.91	157	248	6.91	111	203	1.21	167	259	4.64
192	281	7.23	148	238	6.84	204	294	2.67	158	249	6.66	112	204	1.14	168	260	4.70
193	282	6.84	149	239	7.35	205	295	2.78	159	250	6.67	113	205	1.74	169	261	4.89
194	283	6.29	150	240	7.53	206	296	2.87	160	251	6.34	114	206	2.27	170	262	4.95
195	284	5.97	151	241	8.00	207	297	3.12	161	252	6.35	115	207	3.24	171	263	5.33
196	285	5.56	152	242	7.97	208	298	3.17	162	253	6.05	116	208	3.84	172	264	5.59
197	286	5.30	153	243	7.89	209	299	3.03	163	254	5.87	117	209	4.59	173	265	5.67
198	287	4.86	154	244	7.61	$Z = 91$ (Pa)			164	255	5.58	118	210	5.44	174	266	5.74
199	288	4.39	155	245	7.36	109	200	2.18	165	256	5.35	119	211	6.51	175	267	6.11
200	289	3.81	156	246	6.94	110	201	2.08	166	257	5.17	120	212	7.18	176	268	6.60
201	290	3.41	157	247	7.12	111	202	2.06	167	258	5.30	121	213	7.85	177	269	7.03
202	291	3.00	158	248	6.88	112	203	2.08	168	259	5.42	122	214	8.30	178	270	7.09
203	292	2.82	159	249	6.72	113	204	2.64	169	260	5.64	123	215	8.82	179	271	7.58

TABLE I. (*Continued.*)

N	A	B_f (MeV)	N	A	B_f (MeV)	N	A	B_f (MeV)	N	A	B_f (MeV)	N	A	B_f (MeV)	N	A	B_f (MeV)
$Z = 92$ (U)			$Z = 93$ (Np)			$Z = 93$ (Np)			$Z = 94$ (Pu)			$Z = 94$ (Pu)			$Z = 95$ (Am)		
180	272	7.64	134	227	3.78	190	283	4.90	144	238	5.26	200	294	4.03	153	248	6.91
181	273	8.06	135	228	3.70	191	284	5.12	145	239	5.74	201	295	3.84	154	249	6.59
182	274	8.06	136	229	3.81	192	285	5.11	146	240	5.98	202	296	3.51	155	250	6.37
183	275	8.26	137	230	3.81	193	286	5.37	147	241	6.35	203	297	3.34	156	251	5.87
184	276	7.72	138	231	3.81	194	287	5.26	148	242	6.41	204	298	3.04	157	252	5.79
185	277	6.71	139	232	4.14	195	288	5.43	149	243	6.66	205	299	3.18	158	253	5.41
186	278	6.26	140	233	4.37	196	289	4.96	150	244	6.59	206	300	3.28	159	254	5.45
187	279	5.64	141	234	4.63	197	290	4.73	151	245	6.93	207	301	3.58	160	255	5.19
188	280	5.51	142	235	4.83	198	291	4.52	152	246	7.07	208	302	3.69	161	256	5.17
189	281	5.59	143	236	4.81	199	292	4.34	153	247	7.12	209	303	3.89	162	257	4.89
190	282	5.50	144	237	4.94	200	293	4.09	154	248	6.80	210	304	3.96	163	258	4.59
191	283	5.59	145	238	5.36	201	294	3.93	155	249	6.59	211	305	4.15	164	259	4.07
192	284	5.41	146	239	5.57	202	295	3.54	156	250	6.17	212	306	4.22	165	260	4.00
193	285	5.63	147	240	6.01	203	296	3.26	157	251	5.94	213	307	4.40	166	261	3.86
194	286	5.69	148	241	6.15	204	297	3.07	158	252	5.63	214	308	4.34	167	262	3.99
195	287	5.50	149	242	6.76	205	298	3.22	159	253	5.64	215	309	4.36	168	263	3.92
196	288	5.09	150	243	6.87	206	299	3.26	160	254	5.41	216	310	4.12	169	264	4.17
197	289	4.86	151	244	7.35	207	300	3.44	161	255	5.40	217	311	4.20	170	265	4.01
198	290	4.44	152	245	7.27	208	301	3.40	162	256	5.14	218	312	4.10	171	266	4.24
199	291	4.28	153	246	7.39	209	302	3.48	163	257	4.83	$Z = 95$ (Am)			172	267	4.48
200	292	3.93	154	247	7.09	210	303	3.50	164	258	4.27	117	212	2.40	173	268	4.51
201	293	3.84	155	248	6.89	211	304	3.66	165	259	4.04	118	213	3.13	174	269	4.48
202	294	3.33	156	249	6.46	212	305	3.65	166	260	3.96	119	214	3.57	175	270	4.88
203	295	3.12	157	250	6.35	213	306	3.85	167	261	4.09	120	215	4.03	176	271	5.26
204	296	2.95	158	251	6.01	214	307	3.83	168	262	3.94	121	216	4.56	177	272	5.62
205	297	3.02	159	252	5.87	215	308	4.08	169	263	4.10	122	217	4.81	178	273	5.56
206	298	3.16	160	253	5.72	$Z = 94$ (Pu)			170	264	3.91	123	218	5.32	179	274	5.81
207	299	3.40	161	254	5.64	115	209	1.72	171	265	4.24	124	219	5.60	180	275	5.61
208	300	3.38	162	255	5.39	116	210	2.25	172	266	4.59	125	220	6.19	181	276	5.85
209	301	3.33	163	256	5.12	117	211	3.05	173	267	4.63	126	221	6.23	182	277	5.49
210	302	3.20	164	257	4.58	118	212	3.59	174	268	4.70	127	222	5.46	183	278	5.08
211	303	3.24	165	258	4.27	119	213	4.39	175	269	5.27	128	223	4.74	184	279	4.64
212	304	3.23	166	259	4.06	120	214	5.09	176	270	5.74	129	224	4.33	185	280	4.08
213	305	3.44	167	260	4.04	121	215	5.70	177	271	6.21	130	225	3.80	186	281	3.52
$Z = 93$ (Np)			168	261	4.04	122	216	6.01	178	272	6.18	131	226	3.61	187	282	3.63
113	206	1.16	169	262	4.18	123	217	6.45	179	273	6.32	132	227	2.91	188	283	3.46
114	207	1.66	170	263	4.17	124	218	6.78	180	274	6.20	133	228	2.71	189	284	3.71
115	208	2.52	171	264	4.76	125	219	7.28	181	275	6.35	134	229	2.50	190	285	3.74
116	209	3.05	172	265	5.12	126	220	7.34	182	276	6.15	135	230	2.46	191	286	3.97
117	210	3.72	173	266	5.23	127	221	6.44	183	277	6.07	136	231	2.51	192	287	3.95
118	211	4.49	174	267	5.29	128	222	5.62	184	278	5.72	137	232	2.65	193	288	4.20
119	212	5.21	175	268	5.78	129	223	5.07	185	279	4.96	138	233	2.79	194	289	4.19
120	213	6.09	176	269	6.18	130	224	4.47	186	280	4.43	139	234	3.27	195	290	4.69
121	214	6.67	177	270	6.60	131	225	4.24	187	281	4.12	140	235	3.80	196	291	4.61
122	215	7.00	178	271	6.51	132	226	3.74	188	282	4.07	141	236	4.33	197	292	4.76
123	216	7.52	179	272	6.68	133	227	3.43	189	283	4.29	142	237	4.80	198	293	4.61
124	217	7.83	180	273	6.56	134	228	2.93	190	284	4.24	143	238	5.34	199	294	4.40
125	218	8.28	181	274	7.01	135	229	2.95	191	285	4.47	144	239	5.66	200	295	4.15
126	219	8.26	182	275	6.93	136	230	3.07	192	286	4.49	145	240	6.12	201	296	3.96
127	220	7.32	183	276	7.01	137	231	3.05	193	287	4.69	146	241	6.34	202	297	3.66
128	221	6.47	184	277	6.43	138	232	3.23	194	288	4.59	147	242	6.72	203	298	3.53
129	222	6.01	185	278	5.72	139	233	3.50	195	289	4.73	148	243	6.80	204	299	3.34
130	223	5.28	186	279	5.19	140	234	3.83	196	290	4.65	149	244	6.99	205	300	3.60
131	224	4.96	187	280	5.08	141	235	4.09	197	291	4.68	150	245	6.80	206	301	3.69
132	225	4.43	188	281	4.79	142	236	4.49	198	292	4.47	151	246	6.88	207	302	3.99
133	226	4.17	189	282	5.00	143	237	5.00	199	293	4.32	152	247	6.83	208	303	4.11

TABLE I. (*Continued.*)

N	A	B_f (MeV)	N	A	B_f (MeV)	N	A	B_f (MeV)	N	A	B_f (MeV)	N	A	B_f (MeV)	N	A	B_f (MeV)
$Z = 95$ (Am)			$Z = 96$ (Cm)			$Z = 96$ (Cm)			$Z = 97$ (Bk)			$Z = 98$ (Cf)			$Z = 98$ (Cf)		
209	304	4.33	162	258	4.69	218	314	4.31	171	268	4.07	123	221	3.09	179	277	4.68
210	305	4.43	163	259	4.37	219	315	4.28	172	269	4.09	124	222	3.39	180	278	4.47
211	306	4.62	164	260	4.15	220	316	4.14	173	270	4.32	125	223	3.89	181	279	4.65
212	307	4.64	165	261	4.07	221	317	4.18	174	271	4.19	126	224	4.04	182	280	4.53
213	308	4.66	166	262	3.88	222	318	3.97	175	272	4.33	127	225	3.41	183	281	4.47
214	309	4.44	167	263	3.92	$Z = 97$ (Bk)			176	273	4.49	128	226	2.65	184	282	3.82
215	310	4.42	168	264	3.85	121	218	2.90	177	274	4.77	129	227	1.99	185	283	2.86
216	311	4.20	169	265	4.01	122	219	3.16	178	275	4.69	130	228	1.39	186	284	2.00
217	312	4.25	170	266	3.99	123	220	3.65	179	276	4.93	131	229	1.58	187	285	1.50
218	313	4.16	171	267	4.32	124	221	3.93	180	277	4.71	132	230	1.58	188	286	1.27
219	314	4.18	172	268	4.40	125	222	4.49	181	278	4.86	133	231	1.67	189	287	1.51
220	315	4.01	173	269	4.53	126	223	4.66	182	279	4.70	134	232	1.57	190	288	1.70
$Z = 96$ (Cm)			174	270	4.45	127	224	3.98	183	280	4.61	135	233	1.50	191	289	2.00
119	215	3.04	175	271	4.65	128	225	3.44	184	281	3.87	136	234	1.64	192	290	2.21
120	216	3.31	176	272	4.95	129	226	2.84	185	282	2.95	137	235	2.10	193	291	2.52
121	217	3.78	177	273	5.22	130	227	2.17	186	283	2.17	138	236	2.69	194	292	2.69
122	218	4.09	178	274	5.17	131	228	2.17	187	284	2.09	139	237	3.34	195	293	3.05
123	219	4.59	179	275	5.45	132	229	1.93	188	285	2.00	140	238	4.01	196	294	3.21
124	220	4.99	180	276	5.33	133	230	1.72	189	286	2.29	141	239	4.64	197	295	3.59
125	221	5.62	181	277	5.53	134	231	1.64	190	287	2.43	142	240	5.22	198	296	3.73
126	222	5.64	182	278	5.34	135	232	1.81	191	288	2.70	143	241	5.83	199	297	3.94
127	223	4.85	183	279	5.13	136	233	1.94	192	289	2.84	144	242	6.16	200	298	3.85
128	224	4.16	184	280	4.40	137	234	2.27	193	290	3.13	145	243	6.55	201	299	4.04
129	225	3.69	185	281	3.31	138	235	2.71	194	291	3.33	146	244	6.69	202	300	4.10
130	226	3.02	186	282	2.84	139	236	3.37	195	292	3.68	147	245	6.99	203	301	4.27
131	227	2.68	187	283	2.72	140	237	3.99	196	293	3.85	148	246	7.16	204	302	4.28
132	228	2.11	188	284	2.59	141	238	4.55	197	294	4.21	149	247	7.35	205	303	4.43
133	229	1.99	189	285	2.85	142	239	5.16	198	295	4.10	150	248	7.24	206	304	4.48
134	230	1.87	190	286	2.81	143	240	5.76	199	296	4.14	151	249	7.31	207	305	4.62
135	231	2.00	191	287	3.05	144	241	6.14	200	297	3.98	152	250	7.09	208	306	4.64
136	232	2.10	192	288	3.14	145	242	6.63	201	298	4.05	153	251	6.64	209	307	4.86
137	233	2.24	193	289	3.41	146	243	6.91	202	299	3.99	154	252	6.07	210	308	4.81
138	234	2.61	194	290	3.58	147	244	7.28	203	300	4.17	155	253	5.62	211	309	4.91
139	235	3.23	195	291	3.97	148	245	7.22	204	301	4.20	156	254	5.27	212	310	4.76
140	236	3.81	196	292	4.14	149	246	7.32	205	302	4.42	157	255	5.21	213	311	4.83
141	237	4.34	197	293	4.45	150	247	7.18	206	303	4.43	158	256	4.82	214	312	4.56
142	238	4.92	198	294	4.26	151	248	7.27	207	304	4.59	159	257	4.56	215	313	4.62
143	239	5.48	199	295	4.26	152	249	7.00	208	305	4.66	160	258	4.43	216	314	4.47
144	240	5.85	200	296	4.01	153	250	6.59	209	306	4.95	161	259	4.57	217	315	4.56
145	241	6.32	201	297	3.89	154	251	6.21	210	307	4.90	162	260	4.64	218	316	4.50
146	242	6.56	202	298	3.61	155	252	6.01	211	308	4.99	163	261	4.54	219	317	4.49
147	243	6.97	203	299	3.78	156	253	5.59	212	309	4.84	164	262	4.30	220	318	4.30
148	244	6.92	204	300	3.87	157	254	5.50	213	310	4.82	165	263	4.06	221	319	4.30
149	245	7.13	205	301	4.02	158	255	5.10	214	311	4.70	166	264	3.81	222	320	4.18
150	246	7.02	206	302	4.11	159	256	5.09	215	312	4.61	167	265	3.77	223	321	4.11
151	247	7.11	207	303	4.38	160	257	4.80	216	313	4.44	168	266	3.68	224	322	3.86
152	248	6.80	208	304	4.49	161	258	4.58	217	314	4.53	169	267	3.64	225	323	3.84
153	249	6.56	209	305	4.70	162	259	4.51	218	315	4.45	170	268	3.65	226	324	4.02
154	250	6.25	210	306	4.84	163	260	4.42	219	316	4.45	171	269	3.98	227	325	3.86
155	251	6.09	211	307	4.91	164	261	4.21	220	317	4.28	172	270	4.09	$Z = 99$ (Es)		
156	252	5.68	212	308	4.75	165	262	4.03	221	318	4.31	173	271	4.27	125	224	2.29
157	253	5.57	213	309	4.72	166	263	3.80	222	319	4.08	174	272	4.18	126	225	2.51
158	254	5.20	214	310	4.51	167	264	3.80	223	320	4.06	175	273	4.11	127	226	1.80
159	255	5.22	215	311	4.48	168	265	3.72	224	321	3.78	176	274	4.30	128	227	0.98
160	256	5.00	216	312	4.34	169	266	3.74				177	275	4.56	129	228	1.01
161	257	4.97	217	313	4.42	170	267	3.70				178	276	4.50	130	229	0.70

TABLE I. (*Continued.*)

N	A	B_f (MeV)	N	A	B_f (MeV)	N	A	B_f (MeV)	N	A	B_f (MeV)	N	A	B_f (MeV)	N	A	B_f (MeV)
$Z = 99$ (Es)			$Z = 99$ (Es)			$Z = 100$ (Fm)			$Z = 100$ (Fm)			$Z = 101$ (Md)			$Z = 101$ (Md)		
131	230	1.30	187	286	1.46	138	238	2.88	194	294	2.66	146	247	5.74	202	303	4.31
132	231	1.30	188	287	1.21	139	239	3.49	195	295	2.87	147	248	6.03	203	304	4.46
133	232	1.44	189	288	1.40	140	240	4.14	196	296	2.99	148	249	6.24	204	305	4.38
134	233	1.46	190	289	1.63	141	241	4.50	197	297	3.23	149	250	6.70	205	306	4.39
135	234	1.56	191	290	1.80	142	242	4.88	198	298	3.48	150	251	6.98	206	307	4.41
136	235	1.83	192	291	2.06	143	243	5.29	199	299	3.86	151	252	7.23	207	308	4.39
137	236	2.38	193	292	2.39	144	244	5.57	200	300	4.00	152	253	7.01	208	309	4.29
138	237	2.96	194	293	2.57	145	245	5.94	201	301	4.23	153	254	6.61	209	310	4.32
139	238	3.59	195	294	2.77	146	246	6.13	202	302	4.29	154	255	6.13	210	311	4.36
140	239	4.32	196	295	3.00	147	247	6.48	203	303	4.44	155	256	5.69	211	312	4.50
141	240	4.95	197	296	3.22	148	248	6.73	204	304	4.34	156	257	5.09	212	313	4.46
142	241	5.32	198	297	3.42	149	249	7.12	205	305	4.41	157	258	4.84	213	314	4.59
143	242	5.70	199	298	3.76	150	250	7.22	206	306	4.46	158	259	4.67	214	315	4.54
144	243	5.98	200	299	3.95	151	251	7.38	207	307	4.52	159	260	4.92	215	316	4.63
145	244	6.28	201	300	4.21	152	252	7.16	208	308	4.41	160	261	4.99	216	317	4.52
146	245	6.53	202	301	4.26	153	253	6.74	209	309	4.50	161	262	5.05	217	318	4.68
147	246	6.90	203	302	4.42	154	254	6.24	210	310	4.50	162	263	5.12	218	319	4.62
148	247	7.07	204	303	4.42	155	255	5.72	211	311	4.60	163	264	4.89	219	320	4.71
149	248	7.44	205	304	4.53	156	256	5.11	212	312	4.52	164	265	4.59	220	321	4.75
150	249	7.38	206	305	4.59	157	257	4.75	213	313	4.66	165	266	4.31	221	322	4.90
151	250	7.48	207	306	4.70	158	258	4.52	214	314	4.54	166	267	3.99	222	323	4.81
152	251	7.24	208	307	4.67	159	259	4.54	215	315	4.63	167	268	3.75	223	324	4.79
153	252	6.79	209	308	4.73	160	260	4.62	216	316	4.50	168	269	3.57	224	325	4.47
154	253	6.22	210	309	4.72	161	261	4.68	217	317	4.63	169	270	3.54	225	326	4.57
155	254	5.67	211	310	4.80	162	262	4.82	218	318	4.55	170	271	3.47	226	327	4.42
156	255	5.05	212	311	4.68	163	263	4.75	219	319	4.57	171	272	3.75	227	328	4.91
157	256	5.01	213	312	4.78	164	264	4.49	220	320	4.58	172	273	3.77	228	329	4.62
158	257	4.50	214	313	4.67	165	265	4.23	221	321	4.76	173	274	3.99	229	330	4.66
159	258	4.32	215	314	4.70	166	266	3.94	222	322	4.51	174	275	3.92	$Z = 102$ (No)		
160	259	4.43	216	315	4.57	167	267	3.74	223	323	4.53	175	276	4.00	130	232	0.83
161	260	4.64	217	316	4.67	168	268	3.60	224	324	4.20	176	277	3.67	131	233	0.75
162	261	4.68	218	317	4.55	169	269	3.58	225	325	4.27	177	278	3.85	132	234	0.97
163	262	4.60	219	318	4.57	170	270	3.58	226	326	4.11	178	279	3.72	133	235	1.03
164	263	4.32	220	319	4.39	171	271	3.87	227	327	4.51	179	280	3.95	134	236	1.27
165	264	4.06	221	320	4.56	172	272	3.91	228	328	4.25	180	281	3.72	135	237	1.59
166	265	3.81	222	321	4.39	173	273	4.14	229	329	4.32	181	282	3.78	136	238	2.05
167	266	3.71	223	322	4.25	174	274	4.06	230	330	3.98	182	283	3.52	137	239	2.35
168	267	3.60	224	323	4.01	175	275	4.12	$Z = 101$ (Md)			183	284	3.60	138	240	2.55
169	268	3.51	225	324	4.01	176	276	3.77	128	229	0.70	184	285	3.11	139	241	2.82
170	269	3.50	226	325	3.83	177	277	4.13	129	230	0.84	185	286	2.37	140	242	3.18
171	270	3.82	227	326	4.12	178	278	4.06	130	231	0.74	186	287	1.53	141	243	3.58
172	271	3.85	228	327	3.74	179	279	4.25	131	232	0.89	187	288	1.26	142	244	3.94
173	272	4.08	229	328	3.91	180	280	4.03	132	233	1.03	188	289	1.15	143	245	4.32
174	273	3.96	$Z = 100$ (Fm)			181	281	4.13	133	234	1.30	189	290	1.38	144	246	4.62
175	274	4.06	126	226	2.84	182	282	3.93	134	235	1.57	190	291	1.71	145	247	4.98
176	275	3.82	127	227	2.08	183	283	3.96	135	236	1.72	191	292	1.99	146	248	5.24
177	276	4.17	128	228	0.80	184	284	3.43	136	237	2.01	192	293	2.28	147	249	5.61
178	277	4.10	129	229	0.90	185	285	2.58	137	238	2.49	193	294	2.63	148	250	5.83
179	278	4.27	130	230	0.79	186	286	1.71	138	239	2.86	194	295	2.69	149	251	6.25
180	279	4.02	131	231	0.85	187	287	1.29	139	240	3.25	195	296	2.95	150	252	6.50
181	280	4.12	132	232	1.25	188	288	1.17	140	241	3.64	196	297	3.12	151	253	6.93
182	281	3.95	133	233	1.39	189	289	1.31	141	242	4.09	197	298	3.49	152	254	6.76
183	282	3.99	134	234	1.46	190	290	1.61	142	243	4.46	198	299	3.74	153	255	6.38
184	283	3.39	135	235	1.56	191	291	1.85	143	244	4.80	199	300	3.97	154	256	5.94
185	284	2.60	136	236	1.87	192	292	2.13	144	245	5.11	200	301	4.13	155	257	5.52
186	285	1.75	137	237	2.39	193	293	2.47	145	246	5.47	201	302	4.36	156	258	4.98

TABLE I. (*Continued.*)

N	A	B_f (MeV)	N	A	B_f (MeV)	N	A	B_f (MeV)	N	A	B_f (MeV)	N	A	B_f (MeV)	N	A	B_f (MeV)
$Z = 102$ (No)			$Z = 102$ (No)			$Z = 103$ (Lr)			$Z = 103$ (Lr)			$Z = 104$ (Rf)			$Z = 105$ (Db)		
157	259	5.00	213	315	4.39	171	274	3.94	227	330	6.00	188	292	1.11	152	257	6.22
158	260	4.93	214	316	4.38	172	275	3.94	$Z = 104$ (Rf)			189	293	1.24	153	258	6.01
159	261	5.26	215	317	4.49	173	276	4.21	134	238	1.11	190	294	1.27	154	259	5.76
160	262	5.11	216	318	4.44	174	277	4.13	135	239	1.28	191	295	1.61	155	260	5.81
161	263	5.26	217	319	4.58	175	278	4.23	136	240	1.53	192	296	1.94	156	261	5.76
162	264	5.36	218	320	4.56	176	279	3.87	137	241	1.67	193	297	2.24	157	262	5.94
163	265	5.40	219	321	4.64	177	280	3.76	138	242	1.82	194	298	2.55	158	263	5.90
164	266	5.01	220	322	4.78	178	281	3.65	139	243	2.01	195	299	2.70	159	264	6.08
165	267	4.72	221	323	5.08	179	282	3.91	140	244	2.28	196	300	3.12	160	265	6.36
166	268	4.19	222	324	4.99	180	283	3.62	141	245	2.54	197	301	3.42	161	266	6.80
167	269	3.96	223	325	4.98	181	284	3.86	142	246	2.95	198	302	3.57	162	267	6.99
168	270	3.74	224	326	4.82	182	285	3.58	143	247	3.33	199	303	3.80	163	268	7.00
169	271	3.69	225	327	5.06	183	286	3.61	144	248	3.64	200	304	3.90	164	269	6.59
170	272	3.66	226	328	5.00	184	287	2.99	145	249	3.95	201	305	4.09	165	270	6.13
171	273	3.93	227	329	5.50	185	288	2.26	146	250	4.36	202	306	4.11	166	271	5.62
172	274	3.95	228	330	5.07	186	289	1.61	147	251	4.76	203	307	4.34	167	272	5.18
173	275	4.22	$Z = 103$ (Lr)			187	290	1.32	148	252	5.09	204	308	4.18	168	273	4.69
174	276	4.11	132	235	1.07	188	291	1.04	149	253	5.53	205	309	4.11	169	274	4.45
175	277	4.22	133	236	1.18	189	292	1.22	150	254	5.87	206	310	4.01	170	275	4.00
176	278	3.86	134	237	1.44	190	293	1.51	151	255	6.24	207	311	3.93	171	276	4.16
177	279	3.93	135	238	1.75	191	294	1.89	152	256	6.26	208	312	3.86	172	277	4.21
178	280	3.84	136	239	1.95	192	295	2.19	153	257	6.02	209	313	3.89	173	278	4.48
179	281	4.07	137	240	2.12	193	296	2.51	154	258	5.65	210	314	3.88	174	279	4.48
180	282	3.80	138	241	2.28	194	297	2.68	155	259	5.49	211	315	4.01	175	280	4.56
181	283	4.02	139	242	2.46	195	298	2.93	156	260	5.36	212	316	4.03	176	281	4.35
182	284	3.72	140	243	2.79	196	299	3.24	157	261	5.56	213	317	4.24	177	282	4.31
183	285	3.80	141	244	3.18	197	300	3.59	158	262	5.59	214	318	4.31	178	283	4.20
184	286	3.21	142	245	3.49	198	301	3.74	159	263	5.61	215	319	4.50	179	284	4.59
185	287	2.41	143	246	3.89	199	302	4.01	160	264	5.79	216	320	4.46	180	285	4.37
186	288	1.61	144	247	4.19	200	303	4.08	161	265	6.27	217	321	4.61	181	286	4.40
187	289	1.29	145	248	4.50	201	304	4.27	162	266	6.43	218	322	4.56	182	287	3.86
188	290	0.98	146	249	4.81	202	305	4.22	163	267	6.43	219	323	4.93	183	288	3.79
189	291	1.20	147	250	5.26	203	306	4.39	164	268	6.03	220	324	5.09	184	289	3.06
190	292	1.62	148	251	5.55	204	307	4.36	165	269	5.60	221	325	5.41	185	290	2.35
191	293	1.89	149	252	5.97	205	308	4.23	166	270	5.10	222	326	5.40	186	291	1.78
192	294	2.19	150	253	6.27	206	309	4.14	167	271	4.72	223	327	5.58	187	292	0.90
193	295	2.54	151	254	6.70	207	310	4.03	168	272	4.28	224	328	5.55	188	293	1.11
194	296	2.62	152	255	6.60	208	311	3.99	169	273	4.06	225	329	5.76	189	294	1.23
195	297	2.95	153	256	6.27	209	312	4.07	170	274	3.82	226	330	5.68	190	295	1.16
196	298	3.17	154	257	5.90	210	313	4.06	171	275	4.06	$Z = 105$ (Db)			191	296	1.48
197	299	3.54	155	258	5.52	211	314	4.20	172	276	4.10	136	241	1.31	192	297	1.82
198	300	3.66	156	259	5.21	212	315	4.21	173	277	4.43	137	242	1.44	193	298	2.17
199	301	3.86	157	260	5.39	213	316	4.34	174	278	4.37	138	243	1.55	194	299	2.44
200	302	4.06	158	261	5.37	214	317	4.38	175	279	4.45	139	244	1.68	195	300	2.75
201	303	4.30	159	262	5.52	215	318	4.56	176	280	4.10	140	245	1.94	196	301	3.10
202	304	4.19	160	263	5.48	216	319	4.53	177	281	4.17	141	246	2.18	197	302	3.38
203	305	4.42	161	264	5.73	217	320	4.68	178	282	4.12	142	247	2.59	198	303	3.48
204	306	4.23	162	265	5.97	218	321	4.63	179	283	4.43	143	248	2.88	199	304	3.73
205	307	4.24	163	266	6.03	219	322	4.77	180	284	4.22	144	249	3.21	200	305	3.82
206	308	4.12	164	267	5.63	220	323	4.90	181	285	4.19	145	250	3.53	201	306	4.07
207	309	4.12	165	268	5.22	221	324	5.28	182	286	3.95	146	251	4.01	202	307	4.14
208	310	4.11	166	269	4.81	222	325	5.18	183	287	3.96	147	252	4.44	203	308	4.21
209	311	4.12	167	270	4.36	223	326	5.28	184	288	3.23	148	253	4.81	204	309	4.09
210	312	4.15	168	271	3.96	224	327	5.18	185	289	2.38	149	254	5.26	205	310	3.96
211	313	4.30	169	272	3.78	225	328	5.41	186	290	1.80	150	255	5.67	206	311	3.89
212	314	4.27	170	273	3.69	226	329	5.31	187	291	1.37	151	256	6.05	207	312	3.90

TABLE I. (*Continued.*)

N	A	B_f (MeV)	N	A	B_f (MeV)	N	A	B_f (MeV)	N	A	B_f (MeV)	N	A	B_f (MeV)	N	A	B_f (MeV)
$Z = 105$ (Db)			$Z = 106$ (Sg)			$Z = 107$ (Ns)			$Z = 107$ (Ns)			$Z = 108$ (Hs)			$Z = 109$ (Mt)		
208	313	3.82	175	281	5.06	145	252	2.88	201	308	3.62	174	282	5.51	150	259	4.20
209	314	3.87	176	282	4.82	146	253	3.27	202	309	3.75	175	283	5.76	151	260	4.65
210	315	3.89	177	283	4.83	147	254	3.74	203	310	3.80	176	284	5.74	152	261	5.13
211	316	4.05	178	284	4.75	148	255	4.10	204	311	3.79	177	285	6.01	153	262	5.48
212	317	4.10	179	285	5.05	149	256	4.54	205	312	3.75	178	286	5.89	154	263	5.70
213	318	4.31	180	286	4.91	150	257	5.00	206	313	3.61	179	287	6.43	155	264	5.91
214	319	4.31	181	287	4.91	151	258	5.41	207	314	3.57	180	288	6.25	156	265	5.88
215	320	4.40	182	288	4.44	152	259	5.66	208	315	3.51	181	289	6.24	157	266	5.88
216	321	4.47	183	289	4.15	153	260	5.87	209	316	3.69	182	290	5.83	158	267	6.04
217	322	4.60	184	290	3.42	154	261	6.01	210	317	3.76	183	291	5.59	159	268	6.28
218	323	4.85	185	291	2.60	155	262	6.20	211	318	4.00	184	292	5.02	160	269	6.70
219	324	5.30	186	292	1.97	156	263	6.20	212	319	3.99	185	293	4.02	161	270	7.14
220	325	5.43	187	293	0.02	157	264	6.39	213	320	4.13	186	294	3.31	162	271	7.49
221	326	5.77	188	294	0.02	158	265	6.34	214	321	4.03	187	295	2.62	163	272	7.68
222	327	5.74	189	295	1.01	159	266	6.71	215	322	4.07	188	296	0.01	164	273	7.41
223	328	5.99	190	296	1.01	160	267	6.97	216	323	4.13	189	297	0.83	165	274	7.11
224	329	5.92	191	297	1.10	161	268	7.20	217	324	4.61	190	298	0.70	166	275	6.59
225	330	6.18	192	298	1.42	162	269	7.60	218	325	4.97	191	299	0.40	167	276	6.16
$Z = 106$ (Sg)			193	299	1.87	163	270	7.69	219	326	5.52	192	300	0.85	168	277	5.63
138	244	1.15	194	300	2.14	164	271	7.39	220	327	5.69	193	301	1.22	169	278	5.44
139	245	1.27	195	301	2.45	165	272	6.94	221	328	6.02	194	302	1.49	170	279	5.31
140	246	1.44	196	302	2.83	166	273	6.38	222	329	6.15	195	303	1.86	171	280	5.47
141	247	1.73	197	303	3.12	167	274	5.93	223	330	6.50	196	304	2.23	172	281	5.48
142	248	2.11	198	304	3.25	168	275	5.30	$Z = 108$ (Hs)			197	305	2.59	173	282	5.79
143	249	2.38	199	305	3.52	169	276	5.13	142	250	1.02	198	306	2.72	174	283	5.88
144	250	2.67	200	306	3.63	170	277	4.80	143	251	1.55	199	307	2.93	175	284	6.30
145	251	3.16	201	307	3.85	171	278	4.82	144	252	1.97	200	308	3.03	176	285	6.22
146	252	3.59	202	308	3.92	172	279	4.73	145	253	2.39	201	309	3.34	177	286	6.51
147	253	4.02	203	309	4.03	173	280	5.05	146	254	2.82	202	310	3.45	178	287	6.51
148	254	4.44	204	310	3.92	174	281	5.07	147	255	3.22	203	311	3.47	179	288	6.96
149	255	4.86	205	311	3.94	175	282	5.39	148	256	3.64	204	312	3.43	180	289	6.56
150	256	5.30	206	312	3.76	176	283	5.10	149	257	4.01	205	313	3.38	181	290	6.51
151	257	5.70	207	313	3.72	177	284	5.12	150	258	4.54	206	314	3.22	182	291	6.10
152	258	5.93	208	314	3.69	178	285	5.03	151	259	4.93	207	315	3.23	183	292	5.86
153	259	5.82	209	315	3.82	179	286	5.45	152	260	5.39	208	316	3.18	184	293	5.26
154	260	5.84	210	316	3.85	180	287	5.29	153	261	5.65	209	317	3.32	185	294	4.38
155	261	5.88	211	317	4.04	181	288	5.36	154	262	5.88	210	318	3.41	186	295	3.78
156	262	5.91	212	318	4.10	182	289	4.93	155	263	6.01	211	319	3.65	187	296	3.06
157	263	6.17	213	319	4.19	183	290	4.74	156	264	6.13	212	320	3.64	188	297	2.24
158	264	5.98	214	320	4.13	184	291	4.15	157	265	6.26	213	321	3.78	189	298	1.12
159	265	6.27	215	321	4.22	185	292	2.66	158	266	6.26	214	322	3.69	190	299	0.06
160	266	6.69	216	322	4.21	186	293	2.70	159	267	6.47	215	323	3.82	191	300	0.13
161	267	7.08	217	323	4.38	187	294	0.02	160	268	6.59	216	324	3.93	192	301	0.07
162	268	7.29	218	324	4.87	188	295	0.02	161	269	7.04	217	325	4.58	193	302	0.83
163	269	7.30	219	325	5.42	189	296	0.87	162	270	7.37	218	326	4.92	194	303	1.15
164	270	6.92	220	326	5.55	190	297	1.02	163	271	7.49	219	327	5.44	195	304	1.57
165	271	6.48	221	327	5.91	191	298	0.84	164	272	7.30	220	328	5.57	196	305	1.90
166	272	5.94	222	328	5.94	192	299	1.25	165	273	6.93	221	329	5.92	197	306	2.23
167	273	5.48	223	329	6.19	193	300	1.67	166	274	6.45	222	330	6.11	198	307	2.45
168	274	4.96	224	330	6.13	194	301	1.93	167	275	6.08	$Z = 109$ (Mt)			199	308	2.65
169	275	4.70	$Z = 107$ (Ns)			195	302	2.32	168	276	5.52	144	253	1.59	200	309	2.76
170	276	4.39	140	247	1.13	196	303	2.69	169	277	5.68	145	254	1.96	201	310	3.03
171	277	4.43	141	248	1.33	197	304	2.96	170	278	5.50	146	255	2.37	202	311	3.21
172	278	4.39	142	249	1.70	198	305	3.08	171	279	5.18	147	256	2.76	203	312	3.23
173	279	4.63	143	250	1.91	199	306	3.29	172	280	5.27	148	257	3.22	204	313	3.06
174	280	4.63	144	251	2.45	200	307	3.39	173	281	5.62	149	258	3.58	205	314	3.03

TABLE I. (*Continued.*)

N	A	B_f (MeV)	N	A	B_f (MeV)	N	A	B_f (MeV)	N	A	B_f (MeV)	N	A	B_f (MeV)	N	A	B_f (MeV)
$Z = 109$ (Mt)			$Z = 110$ (Ds)			$Z = 111$ (Rg)			$Z = 112$ (Cn)			$Z = 112$ (Cn)			$Z = 113$ (X)		
206	315	2.87	185	295	4.91	167	278	6.06	152	264	3.61	208	320	1.96	197	310	0.79
207	316	2.92	186	296	4.39	168	279	5.70	153	265	3.79	209	321	2.19	198	311	0.85
208	317	2.86	187	297	3.51	169	280	6.01	154	266	4.05	210	322	2.10	199	312	1.26
209	318	3.04	188	298	2.75	170	281	6.03	155	267	4.11	211	323	2.25	200	313	1.70
210	319	3.08	189	299	2.07	171	282	6.37	156	268	4.06	212	324	2.45	201	314	2.00
211	320	3.33	190	300	0.59	172	283	6.64	157	269	4.25	213	325	2.77	202	315	2.11
212	321	3.35	191	301	0.22	173	284	7.26	158	270	4.72	214	326	3.04	203	316	2.22
213	322	3.48	192	302	0.24	174	285	7.55	159	271	5.18	215	327	3.56	204	317	2.09
214	323	3.50	193	303	0.23	175	286	8.06	160	272	5.63	216	328	4.10	205	318	2.12
215	324	3.72	194	304	0.61	176	287	7.87	161	273	6.10	217	329	4.54	206	319	1.91
216	325	4.14	195	305	1.04	177	288	7.90	162	274	6.51	218	330	4.76	207	320	1.95
217	326	4.62	196	306	1.36	178	289	7.98	163	275	6.71	$Z = 113$ (X)			208	321	1.80
218	327	4.99	197	307	1.75	179	290	8.12	164	276	6.59	153	266	3.06	209	322	1.96
219	328	5.44	198	308	2.04	180	291	7.86	165	277	6.36	154	267	3.25	210	323	1.86
220	329	5.48	199	309	2.21	181	292	7.78	166	278	5.99	155	268	3.25	211	324	2.02
221	330	5.83	200	310	2.46	182	293	7.20	167	279	5.78	156	269	3.38	212	325	2.24
$Z = 110$ (Ds)			201	311	2.83	183	294	6.88	168	280	5.89	157	270	3.80	213	326	2.60
146	256	1.76	202	312	2.88	184	295	6.21	169	281	6.25	158	271	4.26	214	327	2.88
147	257	2.12	203	313	2.87	185	296	5.38	170	282	6.51	159	272	4.77	215	328	3.43
148	258	2.68	204	314	2.76	186	297	4.79	171	283	6.99	160	273	5.22	216	329	3.91
149	259	3.15	205	315	2.72	187	298	3.89	172	284	7.41	161	274	5.70	217	330	4.26
150	260	3.70	206	316	2.55	188	299	3.36	173	285	8.00	162	275	6.09	$Z = 114$ (Fl)		
151	261	4.17	207	317	2.56	189	300	2.55	174	286	8.24	163	276	6.38	155	269	2.76
152	262	4.68	208	318	2.46	190	301	1.79	175	287	8.40	164	277	6.31	156	270	2.97
153	263	4.99	209	319	2.65	191	302	1.27	176	288	8.53	165	278	6.06	157	271	3.37
154	264	5.27	210	320	2.68	192	303	0.13	177	289	8.59	166	279	6.12	158	272	3.79
155	265	5.35	211	321	2.88	193	304	0.16	178	290	8.74	167	280	6.41	159	273	4.26
156	266	5.34	212	322	2.98	194	305	0.53	179	291	8.82	168	281	6.66	160	274	4.69
157	267	5.47	213	323	3.19	195	306	0.68	180	292	8.58	169	282	6.98	161	275	5.15
158	268	5.48	214	324	3.26	196	307	0.94	181	293	8.44	170	283	7.35	162	276	5.53
159	269	5.95	215	325	3.67	197	308	1.37	182	294	7.96	171	284	7.93	163	277	5.85
160	270	6.45	216	326	4.02	198	309	1.66	183	295	7.60	172	285	8.33	164	278	6.55
161	271	6.92	217	327	4.53	199	310	1.93	184	296	6.93	173	286	8.72	165	279	6.97
162	272	7.31	218	328	5.03	200	311	2.21	185	297	6.03	174	287	8.75	166	280	7.13
163	273	7.48	219	329	5.04	201	312	2.58	186	298	5.52	175	288	8.92	167	281	7.18
164	274	7.27	220	330	5.39	202	313	2.64	187	299	4.37	176	289	9.14	168	282	7.33
165	275	6.90	$Z = 111$ (Rg)			203	314	2.59	188	300	4.32	177	290	9.28	169	283	7.65
166	276	6.49	148	259	2.32	204	315	2.51	189	301	3.09	178	291	9.33	170	284	8.09
167	277	6.09	149	260	2.71	205	316	2.52	190	302	2.30	179	292	9.44	171	285	8.82
168	278	5.59	150	261	3.20	206	317	2.29	191	303	1.54	180	293	9.05	172	286	9.00
169	279	5.64	151	262	3.62	207	318	2.34	192	304	0.96	181	294	8.88	173	287	9.23
170	280	5.69	152	263	4.21	208	319	2.21	193	305	0.55	182	295	8.34	174	288	9.18
171	281	5.86	153	264	4.42	209	320	2.45	194	306	0.05	183	296	7.97	175	289	9.61
172	282	5.94	154	265	4.75	210	321	2.38	195	307	0.09	184	297	7.26	176	290	9.89
173	283	6.46	155	266	4.72	211	322	2.54	196	308	0.42	185	298	6.42	177	291	9.97
174	284	6.70	156	267	4.80	212	323	2.60	197	309	0.86	186	299	5.89	178	292	9.98
175	285	7.25	157	268	4.88	213	324	2.90	198	310	1.28	187	300	4.79	179	293	9.89
176	286	7.26	158	269	5.10	214	325	3.27	199	311	1.57	188	301	4.20	180	294	9.53
177	287	7.45	159	270	5.70	215	326	3.81	200	312	2.03	189	302	3.76	181	295	9.35
178	288	7.45	160	271	6.13	216	327	4.24	201	313	2.30	190	303	2.93	182	296	8.87
179	289	7.61	161	272	6.62	217	328	4.73	202	314	2.37	191	304	1.92	183	297	8.47
180	290	7.33	162	273	6.96	218	329	4.95	203	315	2.34	192	305	1.34	184	298	7.82
181	291	7.21	163	274	7.20	219	330	5.15	204	316	2.25	193	306	0.73	185	299	6.92
182	292	6.73	164	275	7.01	$Z = 112$ (Cn)			205	317	2.27	194	307	0.50	186	300	6.43
183	293	6.46	165	276	6.71	150	262	2.65	206	318	2.06	195	308	0.31	187	301	5.25
184	294	5.85	166	277	6.37	151	263	3.15	207	319	2.12	196	309	0.37	188	302	4.68

TABLE I. (*Continued.*)

N	A	B_f (MeV)	N	A	B_f (MeV)	N	A	B_f (MeV)	N	A	B_f (MeV)	N	A	B_f (MeV)	N	A	B_f (MeV)
$Z = 114$ (Fl)			$Z = 115$ (X)			$Z = 116$ (Lv)			$Z = 117$ (X)			$Z = 118$ (X)			$Z = 119$ (X)		
189	303	3.50	184	299	7.68	182	298	8.27	183	300	7.42	187	305	3.38	194	313	1.75
190	304	3.68	185	300	6.75	183	299	7.87	184	301	6.78	188	306	2.90	195	314	1.57
191	305	2.36	186	301	6.27	184	300	7.18	185	302	5.83	189	307	2.61	196	315	1.35
192	306	1.83	187	302	5.16	185	301	6.22	186	303	5.35	190	308	2.49	197	316	1.00
193	307	0.94	188	303	4.58	186	302	5.74	187	304	4.24	191	309	2.41	198	317	0.93
194	308	0.71	189	304	3.55	187	303	4.62	188	305	3.66	192	310	1.95	199	318	0.57
195	309	0.53	190	305	2.99	188	304	4.07	189	306	2.66	193	311	1.62	200	319	0.44
196	310	0.57	191	306	2.44	189	305	3.02	190	307	2.26	194	312	1.43	201	320	0.55
197	311	0.74	192	307	1.99	190	306	2.55	191	308	2.04	195	313	1.03	202	321	0.53
198	312	0.79	193	308	1.25	191	307	1.75	192	309	1.77	196	314	0.81	203	322	0.64
199	313	1.04	194	309	1.05	192	308	1.73	193	310	1.35	197	315	0.43	204	323	0.63
200	314	1.47	195	310	0.67	193	309	0.93	194	311	1.07	198	316	0.38	205	324	0.56
201	315	1.74	196	311	0.60	194	310	0.72	195	312	0.48	199	317	0.35	206	325	0.62
202	316	1.92	197	312	0.67	195	311	0.44	196	313	0.24	200	318	0.38	207	326	0.60
203	317	1.97	198	313	0.66	196	312	0.41	197	314	0.43	201	319	0.72	208	327	0.42
204	318	1.91	199	314	0.79	197	313	0.63	198	315	0.49	202	320	0.90	209	328	0.34
205	319	1.85	200	315	1.11	198	314	0.61	199	316	0.50	203	321	0.84	210	329	0.15
206	320	1.46	201	316	1.42	199	315	0.61	200	317	0.50	204	322	0.57	211	330	0.44
207	321	1.45	202	317	1.65	200	316	0.90	201	318	0.89	205	323	0.36	$Z = 120$ (X)		
208	322	1.32	203	318	1.62	201	317	1.28	202	319	1.07	206	324	0.37	167	287	6.35
209	323	1.53	204	319	1.50	202	318	1.47	203	320	0.98	207	325	0.39	168	288	6.85
210	324	1.63	205	320	1.38	203	319	1.36	204	321	0.73	208	326	0.27	169	289	7.35
211	325	1.72	206	321	1.01	204	320	1.16	205	322	0.55	209	327	0.36	170	290	7.70
212	326	2.05	207	322	0.81	205	321	1.09	206	323	0.15	210	328	0.50	171	291	8.26
213	327	2.40	208	323	0.85	206	322	0.63	207	324	0.24	211	329	0.79	172	292	7.36
214	328	2.75	209	324	1.24	207	323	0.53	208	325	0.25	212	330	0.91	173	293	7.44
215	329	3.17	210	325	1.51	208	324	0.63	209	326	0.65	$Z = 119$ (X)			174	294	7.57
216	330	3.50	211	326	1.58	209	325	0.97	210	327	0.79	165	284	5.51	175	295	7.71
$Z = 115$ (X)			212	327	1.76	210	326	1.24	211	328	1.10	166	285	6.19	176	296	7.69
157	272	3.08	213	328	2.10	211	327	1.29	212	329	1.15	167	286	6.70	177	297	7.54
158	273	3.47	214	329	2.50	212	328	1.50	213	330	1.50	168	287	7.34	178	298	7.33
159	274	3.86	215	330	3.08	213	329	1.84	$Z = 118$ (X)			169	288	7.90	179	299	7.48
160	275	4.29	$Z = 116$ (Lv)			214	330	2.20	163	281	4.73	170	289	8.06	180	300	7.01
161	276	4.75	159	275	3.32	$Z = 117$ (X)			164	282	5.49	171	290	7.62	181	301	6.68
162	277	5.20	160	276	3.79	161	278	4.14	165	283	5.88	172	291	7.80	182	302	6.07
163	278	5.61	161	277	4.25	162	279	4.83	166	284	6.31	173	292	8.05	183	303	5.55
164	279	6.51	162	278	4.91	163	280	5.21	167	285	6.85	174	293	8.12	184	304	4.86
165	280	6.70	163	279	5.35	164	281	6.01	168	286	7.37	175	294	8.29	185	305	3.80
166	281	6.82	164	280	6.21	165	282	6.30	169	287	8.12	176	295	8.06	186	306	3.22
167	282	7.18	165	281	6.41	166	283	6.69	170	288	8.32	177	296	8.07	187	307	3.10
168	283	7.60	166	282	6.66	167	284	7.27	171	289	8.85	178	297	7.94	188	308	3.15
169	284	8.18	167	283	7.16	168	285	7.79	172	290	8.39	179	298	8.10	189	309	3.13
170	285	8.58	168	284	7.65	169	286	8.34	173	291	8.41	180	299	7.72	190	310	2.96
171	286	8.96	169	285	8.23	170	287	8.70	174	292	8.41	181	300	7.37	191	311	2.88
172	287	9.20	170	286	8.47	171	288	8.57	175	293	8.53	182	301	6.71	192	312	2.51
173	288	9.42	171	287	8.76	172	289	8.61	176	294	8.48	183	302	6.22	193	313	2.07
174	289	9.29	172	288	9.02	173	290	8.90	177	295	8.46	184	303	5.54	194	314	1.84
175	290	9.53	173	289	8.95	174	291	8.88	178	296	8.36	185	304	4.64	195	315	1.69
176	291	9.60	174	290	8.94	175	292	8.99	179	297	8.49	186	305	4.08	196	316	1.58
177	292	9.76	175	291	9.08	176	293	8.96	180	298	8.05	187	306	2.94	197	317	1.31
178	293	9.87	176	292	9.26	177	294	9.04	181	299	7.76	188	307	3.08	198	318	1.19
179	294	9.93	177	293	9.35	178	295	9.06	182	300	7.15	189	308	3.09	199	319	0.92
180	295	9.57	178	294	9.46	179	296	9.17	183	301	6.67	190	309	2.93	200	320	0.81
181	296	9.36	179	295	9.49	180	297	8.77	184	302	6.01	191	310	2.85	201	321	0.80
182	297	8.81	180	296	9.10	181	298	8.48	185	303	5.08	192	311	2.44	202	322	0.81
183	298	8.38	181	297	8.86	182	299	7.87	186	304	4.54	193	312	1.99	203	323	0.79

TABLE I. (*Continued.*)

N	A	B_f (MeV)	N	A	B_f (MeV)	N	A	B_f (MeV)	N	A	B_f (MeV)	N	A	B_f (MeV)	N	A	B_f (MeV)
$Z = 120$ (X)			$Z = 121$ (X)			$Z = 123$ (X)			$Z = 124$ (X)			$Z = 126$ (X)			$Z = 128$ (X)		
204	324	0.68	208	329	0.17	180	303	5.01	194	318	0.78	184	310	1.80	188	316	2.11
205	325	0.54	209	330	0.70	181	304	4.93	195	319	0.39	185	311	2.08	189	317	2.15
206	326	0.58	$Z = 122$ (X)			182	305	4.25	196	320	0.13	186	312	1.87	190	318	1.93
207	327	0.55	172	294	6.32	183	306	3.69	197	321	0.00	187	313	1.85	191	319	1.57
208	328	0.49	173	295	6.54	184	307	2.95	198	322	0.00	188	314	1.75	192	320	1.26
209	329	0.52	174	296	6.53	185	308	1.94	199	323	0.21	189	315	2.01	193	321	0.93
210	330	0.40	175	297	6.31	186	309	1.14	200	324	0.34	190	316	1.84	194	322	0.67
$Z = 121$ (X)			176	298	6.33	187	310	2.10	201	325	0.47	191	317	1.67	195	323	0.36
169	290	7.07	177	299	6.28	188	311	2.01	202	326	0.43	192	318	1.17	196	324	0.12
170	291	6.46	178	300	6.19	189	312	1.90	203	327	0.48	193	319	0.91	197	325	0.00
171	292	6.82	179	301	6.23	190	313	1.81	204	328	0.37	194	320	0.36	198	326	0.00
172	293	6.89	180	302	5.60	191	314	1.81	205	329	0.36	195	321	0.00	199	327	0.00
173	294	7.31	181	303	5.51	192	315	1.38	206	330	0.16	196	322	0.00	200	328	0.00
174	295	7.03	182	304	4.87	193	316	1.36	$Z = 125$ (X)			197	323	0.00	201	329	0.00
175	296	7.19	183	305	4.33	194	317	1.31	178	303	5.64	198	324	0.00	202	330	0.18
176	297	7.16	184	306	3.62	195	318	1.01	179	304	5.45	199	325	0.00	$Z = 129$ (X)		
177	298	7.05	185	307	2.60	196	319	0.82	180	305	4.93	200	326	0.00	187	316	2.05
178	299	6.99	186	308	1.82	197	320	0.63	181	306	4.44	201	327	0.13	188	317	2.01
179	300	7.10	187	309	2.45	198	321	0.53	182	307	3.71	202	328	0.26	189	318	1.93
180	301	6.66	188	310	2.41	199	322	0.48	183	308	1.81	203	329	0.47	190	319	1.81
181	302	6.31	189	311	2.38	200	323	0.60	184	309	1.08	204	330	0.51	191	320	1.59
182	303	5.64	190	312	2.26	201	324	0.58	185	310	1.96	$Z = 127$ (X)			192	321	1.31
183	304	5.11	191	313	2.25	202	325	0.57	186	311	1.80	183	310	2.63	193	322	1.12
184	305	4.40	192	314	1.82	203	326	0.45	187	312	1.98	184	311	2.08	194	323	0.90
185	306	3.38	193	315	1.54	204	327	0.35	188	313	1.58	185	312	2.15	195	324	0.50
186	307	2.62	194	316	1.46	205	328	0.29	189	314	1.82	186	313	1.93	196	325	0.24
187	308	2.90	195	317	1.18	206	329	0.33	190	315	1.74	187	314	2.02	197	326	0.00
188	309	2.96	196	318	1.18	207	330	0.46	191	316	1.58	188	315	2.07	198	327	0.00
189	310	2.92	197	319	1.02	$Z = 124$ (X)			192	317	1.11	189	316	2.26	199	328	0.00
190	311	2.75	198	320	0.95	176	300	5.64	193	318	0.79	190	317	2.05	200	329	0.00
191	312	2.72	199	321	0.74	177	301	5.77	194	319	0.45	191	318	1.56	201	330	0.00
192	313	2.35	200	322	0.77	178	302	5.63	195	320	0.08	192	319	1.11	$Z = 130$ (X)		
193	314	1.97	201	323	0.74	179	303	5.45	196	321	0.00	193	320	1.00	189	319	2.03
194	315	1.74	202	324	0.66	180	304	4.12	197	322	0.00	194	321	0.47	190	320	1.91
195	316	1.51	203	325	0.48	181	305	3.90	198	323	0.00	195	322	0.12	191	321	1.69
196	317	1.45	204	326	0.46	182	306	3.32	199	324	0.00	196	323	0.00	192	322	1.22
197	318	1.36	205	327	0.35	183	307	2.74	200	325	0.19	197	324	0.00	193	323	1.18
198	319	1.25	206	328	0.38	184	308	2.01	201	326	0.35	198	325	0.00	194	324	0.85
199	320	1.04	207	329	0.49	185	309	1.85	202	327	0.32	199	326	0.00	195	325	0.45
200	321	0.89	208	330	0.41	186	310	1.75	203	328	0.40	200	327	0.00	196	326	0.20
201	322	0.90	$Z = 123$ (X)			187	311	1.74	204	329	0.33	201	328	0.00	197	327	0.03
202	323	0.89	174	297	6.09	188	312	1.66	205	330	0.31	202	329	0.11	198	328	0.00
203	324	0.71	175	298	5.84	189	313	1.45	$Z = 126$ (X)			203	330	0.39	199	329	0.00
204	325	0.62	176	299	5.60	190	314	1.35	180	306	4.69	$Z = 128$ (X)			200	330	0.00
205	326	0.50	177	300	5.54	191	315	1.27	181	307	4.09	185	313	2.00			
206	327	0.57	178	301	5.45	192	316	1.10	182	308	3.51	186	314	1.71			
207	328	0.63	179	302	5.45	193	317	0.96	183	309	2.60	187	315	2.10			

6 MeV above the ground-state minimum, in good agreement with results obtained in our current model [41]. In contrast, Csige and collaborators [42–44] find third minima for nuclei in this region that are up to 3 MeV below the surrounding peaks. We find it difficult to reconcile with potential-energy calculations the substantial difference in barrier structure they find between $^{232}_{92}U_{140}$ [42] and $^{232}_{91}Pa_{141}$ [43] in these studies. A change by just one proton and one neutron cannot, in potential-energy calculations, result in such large differences in barrier structure. For these reasons we refer to Figs. 23–32 in Ref. [1] for a qualitative benchmark of our calculations with respect to barrier parameters derived from analysis of experimental

cross sections, rather than relying on a calculation of an rms deviation between our model calculations and model-dependent "experimental" barrier parameters with inherently similar levels of uncertainty. Such quantitative indicators are easy to misuse for a spurious sense of precision.

Barrier heights have also been estimated from electron-capture (EC) delayed fission data; for some recent discussions, see [1,45,46]. In EC-delayed fission, daughter states up to the EC Q value $Q_{\rm EC}$ are populated. However phase-space properties result in daughter population probabilities that are roughly proportional to $(Q_{\rm EC} - E^*)^5$, where E^* is the excitation energy above the ground state in the daughter. Therefore, the decay intensities to sufficiently high energies so that EC-delayed fission occurs are usually low. For EC-delayed fission to be observable a rough rule of thumb is that

$$Q_{\rm EC} \gtrapprox B_{\rm f} - 2 \ \ {\rm MeV}. \tag{4}$$

We show in Fig. 34 and Table V in Ref. [1] the degree to which our calculated masses and fission-barrier heights satisfy this empirical "rule." With the possible exceptions of a couple of nuclei near $N = 150$, all the observed cases of EC-delayed fission are consistent with our model values. As discussed in Ref. [1], this exception probably occurs because the calculated $N = 150$ neutron gap in the single-particle spectrum in our model is somewhat too large, resulting in too low ground-state energies and slightly too high barriers. But, in general, the relation is well fulfilled in this comparison, which tests the model far from stability, towards the proton-rich side, across the wide region $80 \leqslant Z \leqslant 99$ and $100 \leqslant N \leqslant 150$.

Calculated barrier heights for 3282 nuclides in the heaviest region are plotted in Fig. 1. Above $Z \approx 100$ the macroscopic contribution to the fission barrier is very low. Therefore, survival with respect to spontaneous fission (SF) and the high barriers that are the reason for the long SF half-lives are mainly due to negative ground-state microscopic corrections [47,48], which can be substantial in some localized regions. We observe such localized regions of high fission barriers in the vicinity of $^{252}_{100}{\rm Fm}_{152}$ and $^{270}_{108}{\rm Hs}_{162}$ and in the superheavy-element (SHE) region. In our calculations the maximum ground-state microscopic correction occurs at $Z = 116$ and $N = 178$, rather than at $Z = 114$ and $N = 184$ [6]. The regions of high fission barriers coincide with regions of large ground-state microscopic corrections, which can exceed (in the negative direction) -6 MeV also for deformed nuclei outside the spherical superheavy region near $Z = 114$ and $N = 184$, namely, in the deformed regions centered at $^{252}_{100}{\rm Fm}_{152}$ and $^{270}_{108}{\rm Hs}_{162}$. Along the Fm isotope chain the barrier heights decrease rapidly with distance from $N = 152$, and the spontaneous-fission half-lives show a similar rapid decrease, which is reproduced in numerous calculations, for example Refs. [27,49–53].

In Fig. 2 we display calculated barriers for 2113 nuclei for the lighter region in our study. There is less structure here compared to the heavier region in Fig. 1. In this region, the macroscopic energy contributes significantly to the barrier height, leading to the use of a different energy scale in this figure. Therefore, the only easily discernible shell structure is due to the magic neutron number $N = 126$.

For a long time $Z = 99$ has been the upper limit for reasonably accurate experimental fission-barrier parameters [54–57].

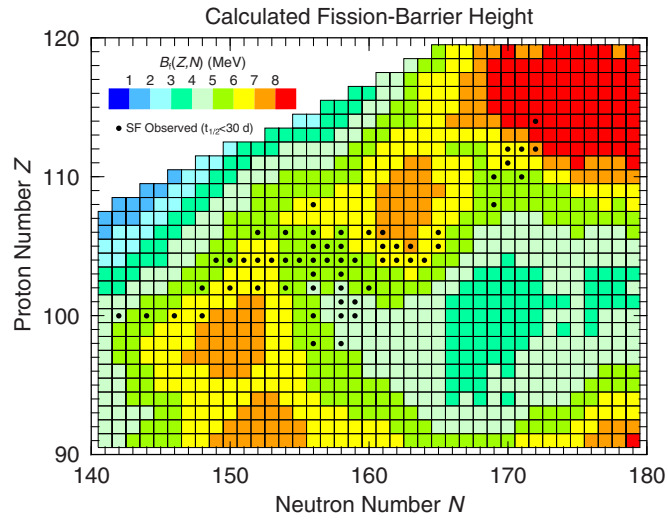

FIG. 4. (Color online) A more detailed look at fission-barrier heights for 980 nuclei in the heaviest region. We have marked with black dots those nuclides for which spontaneous fission with a half-life under about 30 days has been observed.

Only recently has a barrier height for a heavier system, ^{254}No, been determined [58]. However, spontaneous fission has been observed for many heavier systems. We can use these data to further benchmark our calculated barrier heights. In Fig. 4 we show in more detail a limited set of the data in Fig. 1, namely nuclei from the actinide region up to $Z = 119$. We show as black dots those nuclei for which spontaneous fission has been observed with a half-life of less than 30 days, taken from the compilation of Ref. [59]. The aim is to investigate what correlations we find between the calculated barrier heights and the observed fissioning nuclei. This is only to get an overview of the situation because we do not

(i) show that most nuclei in this plot have not been observed experimentally;
(ii) account for the highly variable effect of specialization energies in odd-even and odd-odd nuclei on spontaneous-fission half-lives (this effect can increase half-lives by a factor 10^1 to a factor 10^9 [49]);
(iii) account for the branching ratios between α-decay and fission (for example, a system may have a spontaneous-fission half-life of, say, 1 s, but SF may still not be observed because the α-decay half-life is in the microsecond range).

Despite these limitations we see some interesting correlations that support the accuracy of the calculated barriers. SF is almost exclusively observed in the regions where the predicted barrier is between slightly below 5 and 7 MeV, with only 4 exceptions out of 58 data points. So we conclude from these qualitative arguments that our barrier heights are consistent with the observed occurrences of SF in the heavy-element region.

In some calculations of fission barriers, it is assumed that the shell-plus-pairing corrections at the saddle are small and can be neglected, whereas the shell-plus-pairing

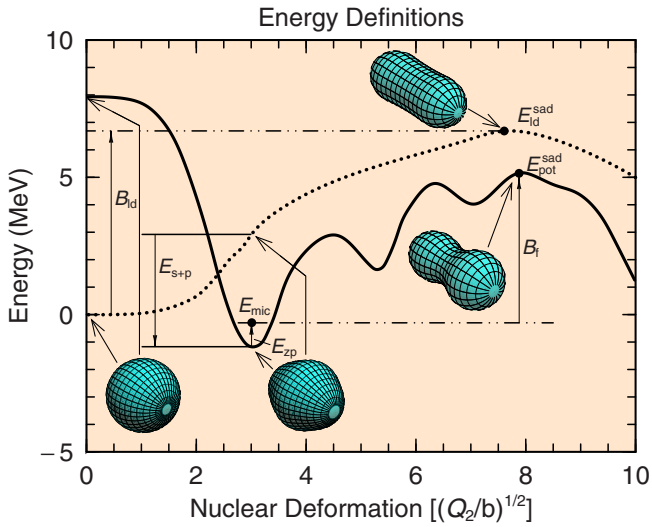

FIG. 5. (Color online) Various energy concepts used in macroscopic-microscopic fission potential-energy calculations. The dotted line is the macroscopic "liquid-drop" energy along a specified path; the solid line is the total macroscopic-microscopic energy along a partially different shape sequence. So that the various energy concepts can be illustrated, the shapes for which the energies have been calculated are as follows. At $Q_2 = 0$ the energies are calculated for a spherical shape. For the shapes from the sphere to the ground-state shape, the shapes are the same for both curves and chosen so that they evolve continuously from the sphere to the calculated macroscopic-microscopic ground-state shape. From the ground state towards larger deformations the total-energy curve is along the optimal fission path that includes all minima and saddle points identified along this path in the five-dimensional deformation space; the liquid-drop-energy curve joins smoothly the macroscopic energy for the shape at the macroscopic-microscopic ground state (which is not the lowest macroscopic energy at this value of Q_2) to the liquid-drop-model saddle point. The energies are calculated for ^{232}Th. Some important shapes are also shown.

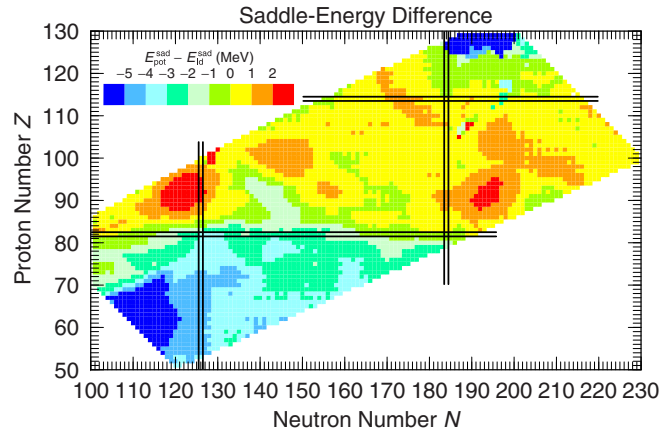

FIG. 6. (Color online) Difference between the saddle-point energy obtained from the five-dimensional macroscopic-microscopic potential-energy surface and the saddle-point energy obtained from a surface in the same deformation space using only the macroscopic model for 5139 nuclei.

corrections at the ground states always have to be included. References [47,48,60] are examples of such studies. We test this assumption below. First, we illustrate some concepts by showing in Fig. 5 a few important quantities and definitions. The total potential energy at a specific shape $E_{\rm pot}$ is the liquid-drop-model energy at this specific shape plus, for the same shape, the shell-plus-pairing correction $E_{\rm s+p}$ (which is negative at the ground state in the case here). To obtain manageable numbers we give all energies relative to the spherical liquid-drop energy, including the liquid-drop energy itself. Therefore, at a specific deformation β (which is a shorthand for any number of deformation parameters, by definition zero for a sphere),

$$E_{\rm pot}(\beta) = E_{\rm ld}(\beta) + E_{\rm s+p}(\beta) - E_{\rm ld}(\beta = 0). \qquad (5)$$

The nuclear mass at the ground state is, in our treatment, the sum of $E_{\rm pot}$ at the ground-state minimum and a zero-point energy [33]. Again, this is relative to the spherical liquid-drop mass (or energy) and is often designated "microscopic correction" $E_{\rm mic}$. The "unnormalized" nuclear mass is therefore the spherical liquid-drop mass plus the microscopic correction. It is thus relative to the potential-energy at the ground state *plus* the zero-point energy that we define the barrier height. By accident, the macroscopic barrier $B_{\rm ld}$ is, in this example, almost the same as $B_{\rm f}$, but generally this is not the case. For ^{208}Pb the difference would be more than 10 MeV due to the large, negative $E_{\rm s+p}$ at the spherical ground-state shape.

We show in Fig. 6 the differences between our saddle-point energies in the macroscopic-microscopic FRLDM model and the saddle-point energies from our macroscopic FRLDM model, both determined in the same five-dimensional space; of course, the shapes of the saddle points in the two models are different. The saddle *energy* differences $E^{\rm sad}_{\rm pot} - E^{\rm sad}_{\rm ld}$ plotted in Fig. 6 are, as postulated, fairly small across large regions of the plot. The rms deviation is 2.25 MeV and the mean deviation (with sign) is −0.78 MeV. In the region of large negative deviations, we find the maximum deviation of −8.45 MeV for $^{171}_{60}$Nd$_{111}$. Why does this large deviation occur here? We calculate the shell-plus-pairing corrections at the saddle-point shape and find it is −8.94 MeV. This saddle-point shape is shown in Fig. 7. It is symmetric and the nascent fragments

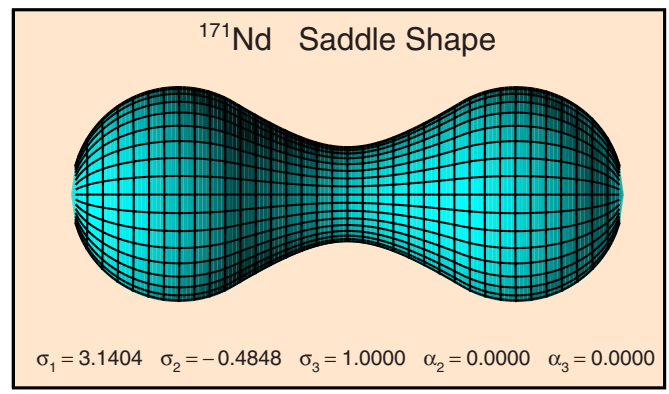

FIG. 7. (Color online) Shape of $^{171}_{60}$Nd$_{111}$ at the saddle point.

are spherical. The fragments are near doubly magic $^{78}_{28}\mathrm{Ni}_{50}$, which in its ground state has a shell+pairing correction of −5.89 MeV. (As shown in Fig. 5, the *microscopic correction* tabulated in Ref. [6] is different from this number.) Twice this number makes −11.78 MeV. The shell-plus-pairing correction we obtain at the saddle point is slightly less negative for a number of reasons. Mainly the shape is not two well-separated Ni nuclei, and the matter in the nascent fragments corresponds to $Z = 26$ and $N = 48$, if the partial spheres are completed to full spheres; the rest of the matter is outside these completed spheres in the neck region. So we now understand why the macroscopic approximation to the saddle energy is of poor accuracy in this particular region. The fragment shell effects dig a deep valley into the potential energy of the compound system in the neighborhood of the saddle point and lower the potential energy by a substantial amount. One may then ask why this does not happen in the actinide region; why does not the shell effect in the doubly magic $^{132}_{50}\mathrm{Sn}_{82}$ (which is −12.82 MeV) affect the saddle-point energy in a similar fashion for actinides? The answer is that the saddle shape of $^{171}_{60}\mathrm{Nd}_{111}$ is much more elongated; $\beta_2 = 2.40$ for this nuclide, whereas for $^{232}_{92}\mathrm{U}_{140}$ and $^{238}_{92}\mathrm{U}_{146}$ we find that $\beta_2 = 1.06$ and $\beta_2 = 0.86$, respectively. For $^{171}_{60}\mathrm{Nd}_{111}$ the saddle shape is very close to the configuration of separated fragments, so the fragment shell effects are almost fully present at the saddle point, while for actinides, though these effects may be present, they are not able to be as fully manifested. Also, when the saddle shape is asymmetric, the macroscopic energy is considerably higher than at the macroscopic, mass-symmetric saddle shape, so this increase in the macroscopic energy cancels a considerable fraction of the "fragment" shell effect. When the saddle shape is symmetric, as is the case for $^{171}_{60}\mathrm{Nd}_{111}$, this does not occur, so the fragment shell effects are more visible at a symmetric saddle than at asymmetric saddle shapes.

When the barrier is very low seemingly "pathological" results can be obtained. For example we find for $^{298}_{108}\mathrm{Hs}_{190}$ that the plotted difference is 7.90 MeV, a very local, surprising, and large deviation. The macroscopic saddle energy is 0.32 MeV and the saddle energy obtained from the macroscopic-microscopic model is 8.22 MeV. To understand these seemingly incompatible results, we show in Fig. 8 the calculated potential-energy surface for $^{298}_{108}\mathrm{Hs}_{190}$, as a function of elongation ϵ_2 and axial asymmetry γ. The details of the calculation and the coordinates are discussed in Ref. [1]. We showed there that for heavy elements one cannot routinely choose as the ground state the lowest minimum in the potential-energy surface because such a minimum may have a very low barrier with respect to fission. Instead, one should choose as the ground state the minimum with the highest barrier with respect to fission, which should have the longest half-life. In this case we identify the minimum at $\epsilon_2 = 0.65$ and $\gamma = 60$ with the ground state and the nearby saddle point indicated by crossed lines, with an energy near 8.2 MeV as the "macroscopic-microscopic" saddle point. Thus, we seem to get a very large failure of the method to use the macroscopic saddle-point energy instead of the "exact" saddle-point energy. However, a very small perturbation of the calculated energies could result in, say, the minimum at

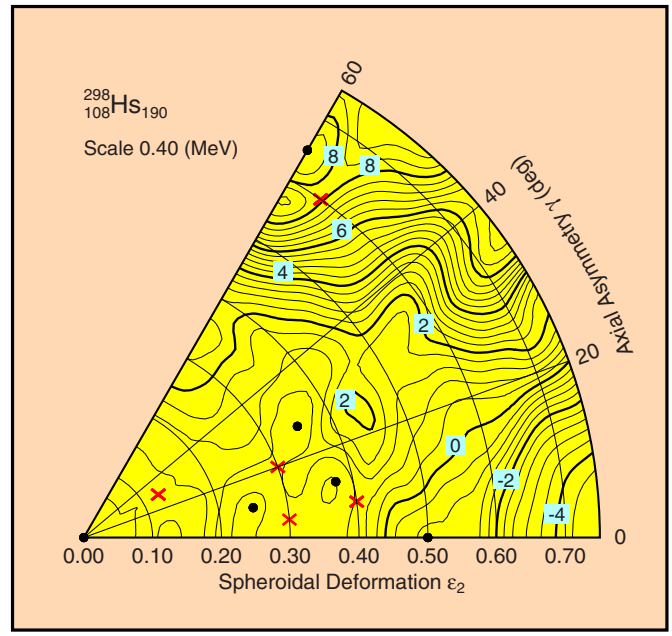

FIG. 8. (Color online) Calculated potential-energy surface for $^{298}_{108}\mathrm{Hs}_{190}$. Local minima are shown by black dots, while saddle points are shown by magenta-colored crosses. The ground state is located at $\gamma = 60$ and $\epsilon_2 = 0.65$, because this is the minimum with the highest barrier with respect to fission; see text for further discussion. But with such a low barrier this isotope would not be observable.

$\epsilon_2 = 0.375$ and $\gamma = 15$ to be identified as the most stable minimum and the nearby saddle at about 0.8 MeV energy to be the macroscopic-microscopic saddle-point energy, now in good agreement with the macroscopic saddle energy. We can summarize these studies as follows.

(1) When discussing the macroscopic approximation to the saddle energy, it is not meaningful to consider nuclei with fission barriers that are so low they would be too unstable to exist. Figure 1 shows that most nuclei slightly above $N = 184$ fall in this category, with some interesting exceptions for low Z and large N.
(2) Above $Z = 80$ and $N \leqslant 184$ the rms deviation between the exact and macroscopic model is 1.12 MeV for the 2433 nuclei in this restricted region. The mean deviation is +0.19 MeV. If all nuclei are included, the rms deviation is 2.25 MeV and the mean deviation is −0.78 MeV, mainly due to the very large negative deviations near $^{171}_{60}\mathrm{Nd}_{111}$.
(3) For systems with $Z < 80$ the macroscopic approximation to the saddle potential energy becomes increasingly inaccurate as Z becomes lower.
(4) Although the macroscopic saddle energy in some regions is a good approximation to the saddle energy obtained in the macroscopic-microscopic model, the shapes associated with the saddle points are very poor approximations to shapes obtained in realistic models. To model fission properties such as low-energy fission-fragment mass distributions, potential-energy surfaces of at least five dimensions calculated either

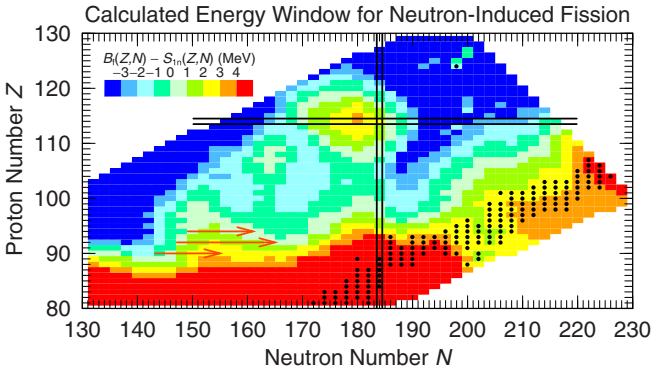

FIG. 9. (Color online) Energy window [6] for neutron-induced fission. The black dots indicate even-N nuclei for which 1.0 MeV $< S_{1n} <$ 2.0 MeV, the so-called r-process boulevard, the region of the chart where the r-process proceeds. If the plotted quantity is negative, the system is unstable with respect to thermal neutron-induced fission. The magenta arrows indicate prompt neutron-capture chains in nuclear-weapons tests; see text for further discussion of this and the single outlying dot at $Z = 124$.

in a macroscopic-microscopic model or some other model with realistic microscopic shell structure are necessary [37–39].

We desire to investigate the accuracy of the calculated barrier heights for neutron-rich nuclei with the aim of understanding their suitability for use in studies such as fission at the end of the r-process. Unfortunately, there are no large-scale systematic experimental studies of fission properties for large regions of nuclei on the neutron-rich side of β-stability. However, some indirect results are available. The r-process can be approximately simulated in certain nuclear explosions through a process called "prompt neutron capture." It is called prompt because the time scale of the neutron fluence is nanoseconds rather than the seconds time scale of the r-process, so the processes are not fully equivalent; no β-decay can occur during the prompt capture due to its short time scale. For a comprehensive discussion of these experiments, see Ref. [61]. Because no β-decay takes place during neutron capture, the process, with some qualifications [61], proceeds along an isotope chain, successively producing increasingly neutron-rich isotopes of a specific element. One necessary condition for the capture sequence to proceed is that the fission barrier be higher than the neutron-separation energy in the compound system following neutron capture. We investigate if our calculations are consistent with experimental observations as regards this necessary condition. In Fig. 9 we show the difference between calculated barrier heights and calculated neutron-separation energies for even systems. Odd compound systems have a (slightly) higher fission barrier and lower neutron-separation energies so they are irrelevant for locating the termination of the capture sequence. Also shown, with magenta arrows, are the "observed" range of neutron-capture chains on the targets $^{232}_{90}$Th$_{142}$, $^{238}_{92}$U$_{146}$, and $^{242}_{94}$Pu$_{148}$. In the uranium chain $^{257}_{92}$U$_{165}$ is reached. This conclusion is not reached by recovering $^{257}_{92}$U$_{165}$ in the debris from the explosion, as it has a calculated β-decay half-life of about 0.5 s [62], too short to allow recovery. Rather, one observes higher-Z, less neutron-rich elements at the end point of β-decay chains from the original isotopes in the capture chain. The termination point of the neutron-capture chain is deduced from the highest A value observed in these groups of nuclei.

From Fig. 9 we see that the observed capture chains for the $^{238}_{92}$U$_{146}$ and $^{242}_{94}$Pu$_{148}$ targets terminate exactly where the plotted function goes below zero, that is, where the fission-barrier height becomes lower than the neutron-separation energy, which would result in termination of the capture sequence by fission. Therefore, the calculated results are consistent with these observations. The capture chain on the $^{232}_{90}$Th$_{142}$ target terminates before zero is reached, but it is argued [61] that this is because the capture cross sections in this chain are very low. So both our calculated barrier heights and neutron-separation energies are consistent with this set of experimental data.

There also could be other mechanisms that cause no nuclei heavier than $A = 257$ to be observed. Nuclei near proton number $Z = 100$ and neutron number $N = 164$ have unusually short half-lives; see Refs. [63,64] for a review and references to original work. The proposed mechanisms for these short half-lives are twofold: (1) a very thin barrier due to "erosion" of the outer barrier due to the large shell effects associated with two near-doubly magic fragments in the vicinity of $^{132}_{50}$Sn$_{82}$ and (2) effects from the large shell gaps on the mass parameter associated with fission. Both of these principles were discussed very early in Ref. [65] and later somewhat more quantitatively in Refs. [5,27,66]. Not many data are available for nuclei in this region but we know for Fm there is a sudden drop in half-life six nucleons (in this case only neutrons) away from $^{264}_{100}$Fm$_{164}$ when we approach this nucleus, which corresponds to doubly magic configurations in both daughter fission fragments in symmetric fission. Since fragment ground-state microscopic corrections near $^{132}_{50}$Sn$_{82}$ decrease in a similar fashion with proton and neutron number variation, we may, as a rule of thumb, anticipate that very short fission half-lives occur at

$$|100 - Z| + |164 - N| \leqslant 6. \quad (6)$$

Thus, even if the actual barriers are higher than the values obtained in our calculations and the capture chain proceeds all the way to $A = 270$, there would be no β-stable products following decay towards stability because the β-decay chains would terminate in fission before relatively stable elements are reached. For instance, suppose $^{260}_{92}$U$_{168}$ is reached. When it decays back, according to the above condition, $^{260}_{95}$Am$_{165}$ would terminate the decay chain by fission. The precursor $^{260}_{94}$Pu$_{166}$ has a calculated β-decay half-life of 0.8 s [62], too short to recover this hypothetical isotope.

In Fig. 9 we have marked even-N nuclides with 1 MeV $< S_{1n} <$ 2 MeV with black dots, defining what is referred to as the r-process boulevard. Along the boulevard the neutron-separation energy is lower than the barrier (although *closer* to stability this is not the case), so according to the results here the r-process can proceed to the heaviest region along this boulevard. However, during β-decay back to stability the decay paths will enter regions with very low barriers so some of the nuclides here will have spontaneous fission half-lives in the microsecond range or lower.

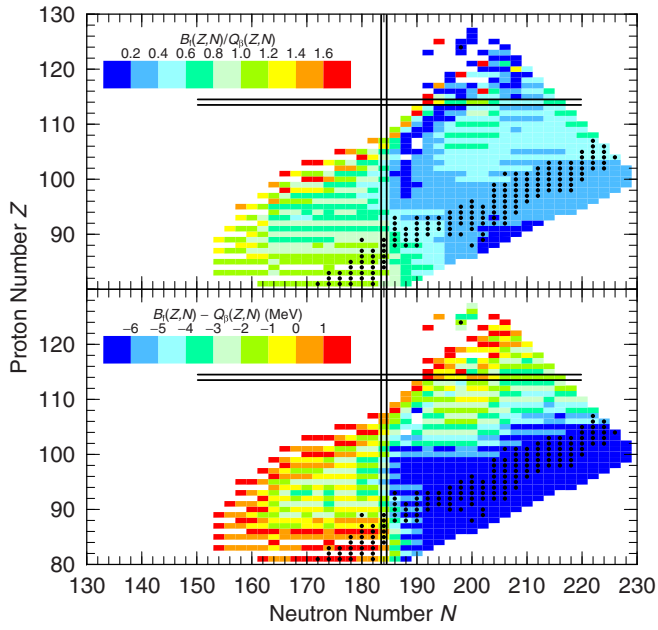

FIG. 10. (Color online) Illustration of quantities affecting β-delayed fission, namely the ratio B_f/Q_β (top panel) and $B_f - Q_\beta$ (bottom panel). Only nuclides for which $B_f - Q_\beta < 2$ MeV are shown. The solid black dots are the same as in Fig. 9, illustrating the "r-process boulevard."

We note that the isolated black dot, indicating that the nuclide at $Z = 124$ and $N = 198$ satisfies the condition which defines the "r-process boulevard," is caused by the phenomenon of highly varying deformations of the ground states in neighboring highly unstable isotopes, due to effects similar to those discussed in reference to Fig. 8.

When the β-decay Q_β value is higher than the fission barrier in the daughter, which is the case across a large region of neutron-rich heavy nuclei, β-delayed fission can occur, sometimes with a high probability. This is illustrated in Fig. 10. The ratio between the barrier height and Q_β is shown in the top panel. Only nuclides for which $B_f - Q_\beta < 2$ MeV are shown, because for decays to energies more than 2 MeV below the barrier peak the delayed fission branch is negligible. Spontaneous fission from the ground state may still occur with a high probability. Smaller ratios correspond to higher probability of delayed fission. As a complementary view we present in the bottom panel the magnitude of the energy window for β-delayed fission. However, the branching ratio for β-delayed fission is not directly related to the magnitude of this window. For example in a decay with a barrier height of, say, $B_f = 2$ MeV and $Q_\beta = 6$ MeV the branching ratio for delayed fission would normally be much larger than if $B_f = 6$ MeV and $Q_\beta = 10$ MeV, although the energy window for delayed fission is 4 MeV in both of these situations.

In summary, we have benchmarked, both previously and in this work, our potential-energy-surface calculations and associated predicted nuclear properties with respect to

(i) barrier heights from $^{70}_{34}Se_{36}$ to $^{252}_{98}Cf_{154}$ [28];
(ii) nuclear ground-state masses [28];
(iii) actinide "double-humped" fission-barrier parameters [1];
(iv) EC-delayed fission data [1,45,46];
(v) spontaneous-fission properties in the heavy-element region;
(vi) fission-fragment charge-yield data for 70 nuclides [39];
(vii) some prompt neutron-capture data obtained in weapons tests.

These studies have been consistently encouraging and represent quite diverse tests, which show that the calculated potential-energy surfaces give a realistic description of available experimental data, including in regions of the nuclear chart far removed from regions considered in determining the parameters of the model. It therefore seems to be very timely to incorporate this calculated fission-barrier-height data base in studies of fission in the r-process. Such studies would require a sophisticated network that should include pathways and branching ratios for neutron capture, neutron-induced fission, β-decay, β-delayed fission, and spontaneous fission. In the fission branches, ideally the fission-fragment yields should also be included.

A computer readable file with the barrier data in Table I is available in Ref. [67]. The format is (Z, N, A, B_f).

ACKNOWLEDGMENTS

This work was supported by travel grants for P.M. to JUSTIPEN (Japan-U.S. Theory Institute for Physics with Exotic Nuclei) under Grant No. DE-FG02-06ER41407 (University of Tennessee). This work was carried out under the auspices of the National Nuclear Security Administration of the U.S. Department of Energy at Los Alamos National Laboratory under Contract No. DE-AC52-06NA25396. T.I. was supported in part by MEXT SPIRE and JICFuS and JSPS KAKENHI Grant No. 25287065. M.M. was supported by the Notre Dame Joint Institute for Nuclear Astrophysics, NSF Grant No. PHY0822648.

[1] P. Möller, A. J. Sierk, T. Ichikawa, A. Iwamoto, R. Bengtsson, H. Uhrenholt, and S. Åberg, Phys. Rev. C **79**, 064304 (2009).
[2] P. Möller and A. Iwamoto, Acta Phys. Hung. New Ser.: Heavy Ion Phys. **10**, 241 (1999).
[3] P. Möller and A. Iwamoto, Phys. Rev. C **61**, 047602 (2000).
[4] P. Möller, D. G. Madland, A. J. Sierk, and A. Iwamoto, AIP Conf. Proc. **561**, 455 (2001).
[5] P. Möller, D. G. Madland, A. J. Sierk, and A. Iwamoto, Nature (London) **409**, 785 (2001).
[6] P. Möller, J. R. Nix, W. D. Myers, and W. J. Swiatecki, At. Data Nucl. Data Tables **59**, 185 (1995).

[7] S. Ćwiok, W. Nazarewicz, J. X. Saladin, W. Plociennik, and A. Johnson, Phys. Lett. B **322**, 304 (1994).
[8] G. M. Ter-Akopian *et al.*, Phys. Rev. Lett. **77**, 32 (1996).
[9] A. Sobiczewski, P. Jachimowicz, and M. Kowal, Int. J. Mod. Phys. E **19**, 493 (2010).
[10] P. Jachimowicz, M. Kowal, and J. Skalski, Phys. Rev. C **85**, 034305 (2012).
[11] H. Flocard, P. Quentin, A. K. Kerman, and D. Vautherin, Nucl. Phys. A **203**, 433 (1973).
[12] B. Hayes, Am. Sci. **88**, 481 (2000).
[13] N. Dubray and D. Regnier, Comput. Phys. Commun. **183**, 2035 (2012).
[14] S. G. Nilsson, Mat.-Fys. Medd. - K. Dan. Vidensk. Selsk. **29**, 16 (1955).
[15] S. G. Nilsson, C. F. Tsang, A. Sobiczewski, Z. Szymański, S. Wycech, C. Gustafson, I.-L. Lamm, P. Möller, and B. Nilsson, Nucl. Phys. A **131**, 1 (1969).
[16] S. Ćwiok, J. Dudek, W. Nazarewicz, J. Skalski, and T. Werner, Comput. Phys. Commun. **46**, 379 (1987).
[17] M. Bolsterli, E. O. Fiset, J. R. Nix, and J. L. Norton, Phys. Rev. C **5**, 1050 (1972).
[18] H. J. Krappe, J. R. Nix, and A. J. Sierk, Phys. Rev. C **20**, 992 (1979).
[19] W. D. Myers and W. J. Swiatecki, Nucl. Phys. **81**, 1 (1966).
[20] W. D. Myers and W. J. Swiatecki, Ark. Fys. **36**, 343 (1967).
[21] K. T. R. Davies, A. J. Sierk, and J. R. Nix, Phys. Rev. C **13**, 2385 (1976).
[22] N. Bohr and J. A. Wheeler, Phys. Rev. **56**, 426 (1939).
[23] O. Hahn and F. Strassmann, Naturwissenschaften **27**, 11 (1939).
[24] L. Meitner and O. R. Frisch, Nature (London) **143**, 239 (1939).
[25] O. R. Frisch, Nature (London) **143**, 276 (1939).
[26] H. A. Bethe and R. F. Bacher, Rev. Mod. Phys. **8**, 82 (1936).
[27] P. Möller, J. R. Nix, and W. J. Swiatecki, Nucl. Phys. A **492**, 349 (1989).
[28] P. Möller, A. J. Sierk, and A. Iwamoto, Phys. Rev. Lett. **92**, 072501 (2004).
[29] W. D. Myers and W. J. Swiatecki, Ann. Phys. (NY) **55**, 395 (1969).
[30] P. Möller and J. R. Nix, *Proceedings of the Third IAEA Symposium on the Physics and Chemistry of Fission, Rochester, 1973* (IAEA, Vienna, 1974), Vol. I, p. 103.
[31] P. Möller and J. R. Nix, Nucl. Phys. A **229**, 269 (1974).
[32] P. Möller, S. G. Nilsson, and J. R. Nix, Nucl. Phys. A **229**, 292 (1974).
[33] P. Möller and J. R. Nix, Nucl. Phys. A **361**, 117 (1981).
[34] P. Möller and J. R. Nix, Nucl. Phys. A **536**, 20 (1992).
[35] P. Möller and S. G. Nilsson, Phys. Lett. B **31**, 283 (1970).
[36] L. Wilets, *Theories of Nuclear Fission* (Clarendon Press, Oxford, 1964).
[37] J. Randrup and P. Möller, Phys. Rev. Lett. **106**, 132503 (2011).
[38] J. Randrup, P. Möller, and A. J. Sierk, Phys. Rev. C **84**, 034613 (2011).
[39] J. Randrup and P. Möller, Phys. Rev. C **88**, 064606 (2013).
[40] J. Blons, R. Fabbro, C. Mazur, D. Paya, M. Ribrag, and Y. Patin, Nucl. Phys. A **477**, 231 (1988).
[41] T. Ichikawa, P. Möller, and A. J. Sierk, Phys. Rev. C **87**, 054326 (2013).
[42] L. Csige, M. Csatlós, T. Faestermann, Z. Gácsi, J. Gulyás, D. Habs, R. Hertenberger, A. Krasznahorkay, R. Lutter, H. J. Maier, P. G. Thirolf, and H.-F. Wirth, Phys. Rev. C **80**, 011301(R) (2009).
[43] L. Csige, M. Csatlós, T. Faestermann, J. Gulyás, D. Habs, R. Hertenberger, M. Hunyadi, A. Krasznahorkay, H. J. Maier, P. G. Thirolf, and H.-F. Wirth, Phys. Rev. C **85**, 054306 (2012).
[44] L. Csige, D. M. Filipescu, T. Glodariu, J. Gulyás, M. M. Günther, D. Habs, H. J. Karwowski, A. Krasznahorkay, G. C. Rich, M. Sin, L. Stroe, O. Tesileanu, and P. G. Thirolf, Phys. Rev. C **87**, 044321 (2013).
[45] A. N. Andreyev, M. Huyse, and P. Van Duppen, Rev. Mod. Phys. **85**, 1541 (2013).
[46] M. Veselský, A. N. Andreyev, S. Antalic, M. Huyse, P. Möller, K. Nishio, A. J. Sierk, P. Van Duppen, and M. Venhart, Phys. Rev. C **86**, 024308 (2012).
[47] W. J. Swiatecki, Phys. Rev. **100**, 937 (1955).
[48] Z. Patyk, A. Sobiczewski, P. Armbruster, and K.-H. Schmidt, Nucl. Phys. A **491**, 267 (1989).
[49] J. Randrup, C. F. Tsang, P. Möller, S. G. Nilsson, and S. E. Larsson, Nucl. Phys. A **217**, 221 (1973).
[50] J. Randrup, S. E. Larsson, P. Möller, S. G. Nilsson, K. Pomorski, and A. Sobiczewski, Phys. Rev. C **13**, 229 (1976).
[51] A. Baran, K. Pomorski, A. Łukasiak, and A. Sobiczewski, Nucl. Phys. A **361**, 83 (1981).
[52] A. Staszczak, A. Baran, J. Dobaczewski, and W. Nazarewicz, Phys. Rev. C **80**, 014309 (2009).
[53] A. Baran, A. Staszczak, and W. Nazarewicz, Int. J. Mod. Phys. E **20**, 557 (2011).
[54] B. B. Back, O. Hansen, H. C. Britt, and J. D. Garrett, Phys. Rev. C **9**, 1924 (1974).
[55] B. B. Back, H. C. Britt, O. Hansen, B. Leroux, and J. D. Garrett, Phys. Rev. C **10**, 1948 (1974).
[56] H. C. Britt, *Proceedings of the 4th IAEA Symposium on the Physics and Chemistry of Fission, Jülich, 1979* (IAEA, Vienna, 1980), Vol. I, p. 3.
[57] S. Bjørnholm and J. E. Lynn, Rev. Mod. Phys. **52**, 725 (1980).
[58] G. Henning *et al.*, Europhys. J. Web Conf. **66**, 02046 (2014).
[59] S. Hofmann, in *Encyclopedia of Nuclear Physics and Its Application*, edited by Reinhard Stock (Wiley-VCH Verlag, Weinheim, Germany, 2013), pp. 213–246.
[60] W. D. Myers and W. J. Swiatecki, Nucl. Phys. A **612**, 249 (1997).
[61] S. A. Becker, *Carnegie Observatories Astrophysics Series*, edited by A. McWilliam and M. Rauch (Carnegie Observatories, Pasadena, CA, 2004), Vol. 4, symposia.obs.carnegiescience.edu/series/symposium4/ms/becker.ps.gz
[62] P. Möller, J. R. Nix, and K.-L. Kratz, At. Data Nucl. Data Tables **66**, 131 (1997).
[63] N. E. Holden and D. C. Hoffman, Pure Appl. Chem. **72**, 1525 (2000).
[64] N. E. Holden and D. C. Hoffman, Pure Appl. Chem. **73**, 1225 (2001).
[65] U. Mosel and H. W. Schmitt, Phys. Rev. C **4**, 2185 (1971).
[66] P. Möller, J. R. Nix, and W. J. Swiatecki, Nucl. Phys. A **469**, 1 (1987).
[67] See Supplemental Material at http://link.aps.org/supplemental/10.1103/PhysRevC.91.024310 for the ASCII version of Table I.